

Single-walled Carbon Nanotubes in Solar Cells

Il Jeon¹ · Yutaka Matsuo^{1,2} · Shigeo Maruyama^{1,3*}

¹ Department of Mechanical Engineering, The University of Tokyo, Tokyo 113-8656, Japan

² Hefei National Laboratory for Physical Sciences at Microscale, University of Science and Technology of China, Anhui 230026, China

³ Energy Nano Engineering Laboratory, National Institute of Advanced Industrial Science and Technology (AIST), Ibaraki 305-8564, Japan

Photovoltaics, more generally known as solar cells, are made from semiconducting materials that convert light into electricity. Solar cells have received much attention in recent years due to their promise as clean and efficient light-harvesting devices. Single-walled carbon nanotubes (SWNTs) could play a crucial role in these devices and have been the subject of much research, which continues to this day. SWNTs are known to outperform multi-walled carbon nanotubes (MWNTs) at low densities, because of the difference in their optical transmittance for the same current density, which is the most important parameter in comparing SWNTs and MWNTs. SWNT films show semiconducting features, which make SWNTs function as active or charge-transporting materials. This chapter, consisting of two sections, focuses on the use of SWNTs in solar cells. In the first section, we discuss SWNTs as a light harvester and charge transporter in the photoactive layer, which are reviewed chronologically to show the history of the research. In the second section, we discuss SWNTs as a transparent conductive layer outside of the photoactive layer, which is relatively more actively researched. This section introduces SWNT applications in silicon solar cells, organic solar cells, and perovskite solar cells each, from their prototypes to recent results. As we go along, the science and prospects of the application of solar cells will be discussed.

1. Single-walled Carbon Nanotubes as the Photoactive Material in Solar Cells

SWNTs provide an ideal light-harvesting medium that has a wide range of direct band gaps,¹ strong absorptions within the solar spectrum,²⁻⁴ and high carrier mobility^{5,6}

with excellent chemical stability. Compared with carbon nanotubes (CNTs), organic compounds have inherently low carrier mobility and low stability. Organic semiconductors have carrier mobility that is hundredth that of inorganic materials. This creates a bottleneck in the performance of organic solar cells (OSCs).⁷⁻¹¹ Therefore, incorporating CNTs in OSCs can improve device performance greatly. In this section, we discuss the use of SWNTs in the photoactive layer of photovoltaics, and review demonstrations of this technology in literature.

An individual SWNT can form a p-n junction diode, giving rise to the photovoltaic effect.^{12,13} Thus, SWNTs exhibit high power conversion efficiency (PCE) under illumination. SWNTs comprise semiconducting and metallic forms, generally in 2 to 1 ratio. Semiconducting SWNTs form Schottky contacts with metallic objects, which are responsible for the ideal diode behavior, whereas metallic SWNTs easily recombine electrons and holes.¹⁴ It is therefore important that SWNTs be purified according to their use. The difference in electronic structure between semiconducting and metallic SWNTs originates from their chirality, and they can be chiral-specifically synthesized^{15,16} or sorted by various methods based on their diameters and electronic properties (Figure 1). Well-known sorting methods are density gradient ultracentrifugation,^{17,18} gel-chromatography,¹⁹ and aqueous two-phase separation²⁰. These methods exploit differences in diameter, chirality, and electronic properties of CNTs to precisely collect multiple chiralities of semiconducting SWNTs. Since each chirality absorbs a specific light wavelength, the semiconducting SWNTs obtained by this method can be used as a photoactive material. Because CNTs have high conductivity along the tube axis, SWNTs can act effectively, not only as a light harvester, but also as a charge transporter in photoactive layer. This means that SWNTs possess dual functionality of a light absorber and a charge-selective material.

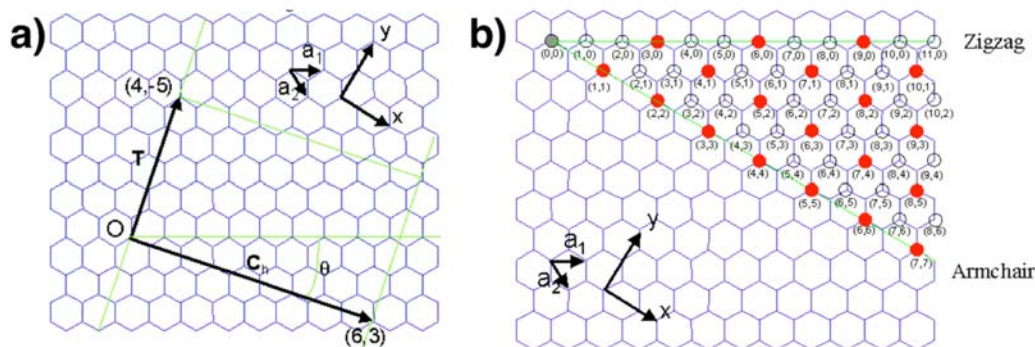


Figure 1. a) Definition of chiral vectors in a hexagonal lattice. b) For a SWNT chirality of (n,m), if the value of $(n-m)/3$ is an integer, the SWNT is metallic. The red dots represent metallic SWNTs.

Solar cell devices, in general, are mainly composed of an active layer, a charge selective layer, and a charge conductive layer. The active layer absorbs light and generates excitons. The charge selective layers are placed above and below the active layer to filter out any unwanted charges to prevent recombination after excitation. These are then followed by the conductive layers, which extract the filtered charges. A polymer matrix composed of conductive polymer, and SWNTs allows exciton dissociation in a strong electric field, with the CNTs functioning as the electron transporter.²¹ An interpenetrating donor–acceptor heterojunction achieves efficient charge separation and charge collection such that electrons and holes can travel toward their respective contacts through the polymers donors and CNT acceptors. Poly(3-hexylthiophene) (P3HT) and poly(3-octylthiophene) (P3OT) are the most commonly used polymer donors and are generally mixed with SWNTs in solution.^{22,23}

1.1 CNT as Electron Acceptors / Transporters

In this line of research, CNTs started out as electron acceptors. Friend and colleagues reported polymer- and CNT-based OSCs using poly(p-phenylene vinylene) (PPV) and MWNTs (Table 1: Report A for the first time to the best of our knowledge.²⁴ Despite effective charge transfer from PPV to the CNTs, charge recombination within the

CNT networks limited the device performance. Moreover, poor dispersion of CNTs in PPV resulted in severe aggregation of the CNTs. Kymakis and Amaratunga reported the OSCs using SWNTs, which were mixed with P3OT (Table 1: Report B).^{21,25} Although the PCE was low (0.04%), they successfully demonstrated the electron acceptor behavior of the SWNTs with an open-circuit voltage (V_{OC}) of 0.9 V and fill factor (FF) of 0.4. The results revealed that photoinduced electron transfer occurred at the polymer/nanotube interface and showed the promise of conjugated polymer-SWNT composites. C₆₀-modified SWNTs were mixed with P3HT to give a much improved PCE of 0.57% (Table 1: Report C).^{26,27} SWNTs and C₆₀ were mixed in toluene and irradiated with microwaves, followed by addition of P3HT. Improved short-circuit current density (J_{SC}) was a direct result of higher electron mobility owing to the SWNTs. Furthermore, a change of morphology increased FF as well.

The thermal post-treatment was discovered at this point, which entails heating devices beyond the glass transition temperature of the polymer donor. This treatment caused beneficial phase separation of the blend and improved the ordering of the polymeric chains, which improved charge transfer, transport, and collection. It was also reported that this treatment substantially increased the hole mobility of the polymer-CNT composites.²⁸ Jousset and colleagues reported SWNT, P3HT, and 1-(3-methoxycarbonyl)-propyl-1-phenyl[6,6]C₆₁ (PCBM) nanocomposites that were prepared by a method using high dissolution followed by concentration to control the ratio of CNTs to P3HT/PCBM in the mixture and disperse the CNTs homogeneously throughout the matrix (Table 1: Report D).⁵ A P3HT/PCBM (1:1) mixture with 0.1 wt % MWNTs gave the highest PCE of 2.0%. Ozkan and colleagues realized controlled placement of an SWNT monolayer network at four different positions in polymer-fullerene solar cells and found that SWNTs on the hole-collecting side of the active layer gave a high PCE of 4.9% (Table 1: Report E) (Figure 2).⁶ They also demonstrated that SWNTs on top of the active layer led to an increased fluorescence lifetime of P3HT. Dip coating from a hydrophilic suspension was used for this experiment. The research of SWNTs as an electron acceptor with Gradecak and co-workers demonstrating SWNT/P3HT bulk heterojunction solar cells with a PCE of 0.72% (Table 1: Report F).²⁹ A key point in this research was using purely semiconducting SWNTs coated with well-ordered P3HT by π -

π interactions to enhance charge separation and transport. They found that the electrical characteristics of the devices were strongly dependent on the SWNT loading. Modeling of the V_{oc} suggested that despite the large carrier mobility in SWNTs, PCE was limited by carrier recombination.

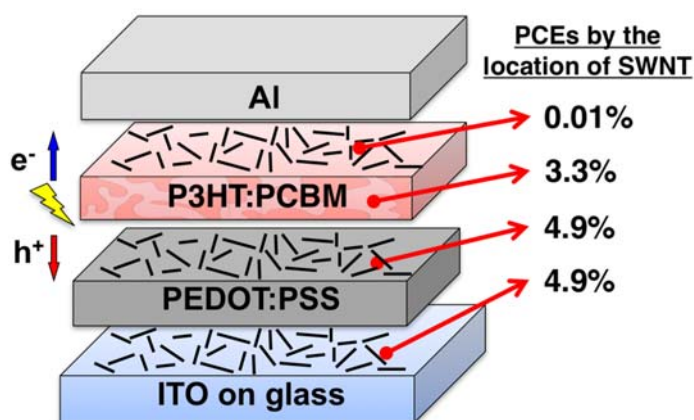


Figure 2. Illustration of a work reported in reference 6. SWNTs located either above or below the hole-transporting layer of OSCs perform the best (the numbers indicate PCEs obtained with different position of the SWNT layer).

1.2 CNT as Light Absorber and Electron Donor

Arnold and colleagues went further and showed that semiconducting SWNTs can be used not only as an electron acceptor but as a light-harvesting electron donor as well.³⁰⁻³² They formed a semiconducting SWNT/PCBM bulk heterojunction with a layer of bathocuproine (BCP) and overcame the limited diffusion of semiconducting SWNTs to produce near-infrared efficiency of 1.3% (Table 1: Report G).³³ A follow-up work,³⁴ provided some mechanistic insights but did not produce a higher efficiency, particularly in the visible region of the solar spectrum. Higher efficiency was not realized until reduced graphene oxide (r-GO) was introduced as a cascade material connecting SWNTs and fullerene acceptors. Both Pristine CNTs and graphene have low surface energy arising from neutral C-C bonding.^{35,36} In contrast, chemically modified graphene, such as r-GO and nitrogen-doped GO, have higher surface energy due to their surface functional

groups and doped heteroatoms with differing electronegativity.³⁷⁻³⁹ With atomic-scale flatness and sufficiently high surface energy, chemically modified graphene adds a robust additional layer to be built upon in further nanoscale processing. The high thermal and chemical stability of chemically modified graphene is advantageous for direct nanoscale processing. Huang and colleagues achieved PCEs of 0.21% and 0.85% using C₆₀ and C₇₀, respectively, in a system, with semiconducting SWNTs as the donor, fullerenes as the acceptor, and r-GO as an energetically mediating species (Table 1: Report H).^{40,41} Ren and colleagues followed suit, but this time, they used r-GO and SWNTs with [6,6]-phenyl C₇₁-butyric acid methyl ester (PC₇₁BM). Also, poly[(9,9-dioctylfluorenyl-2,7-diyl)-co-(4,40-(N-(4-sec-butylphenyl)) diphenylamine)] (TFB) was used as a hole-blocking layer, which is rather unusual. They achieved a PCE of 1.3% using a composition of PC₇₁BM (88-97%)/semiconducting-SWNT (1-10%)/r-GO (~2%) (Table 1: Report I).⁴² Bao and colleagues reported an attempt at an all-carbon OSCs, in which the anode, the active layer, and the cathode were all made up of carbon materials. As a first step, they optimized the active layer composed of a bilayer film of solution-sorted semiconducting SWNTs as the light absorber and donor and C₆₀ as the acceptor between indium tin oxide (ITO) and metal electrodes. By optimizing the semiconducting SWNT dispersion and deposition conditions and the C₆₀ layer thickness, they produced a PCE of 0.46% (Table 1: Report J).^{43,44} As a next step, they replaced the ITO anode with r-GO layers and the metallic cathode with an n-type SWNT film to achieve an all-carbon OSC. However, PCEs were on the order of 0.1%. In 2014, Hersam and colleagues reported a National Renewable Energy Laboratory-certified PCE of 2.5% and a highest PCE of 3.1% using semiconducting SWNTs of various chiralities as the hole-transporting and light-harvesting materials (Table 1: Report K).⁴⁵ Compared with single-chirality semiconducting SWNTs, multi-chirality semiconducting SWNTs enabled a wider range of absorption from visible to near-infrared. Normal and inverted architectures were also fabricated and compared. Inverted architecture gave a higher efficiency owing to ZnO nanowires (NWs) penetrating the active layer (Figure 3).

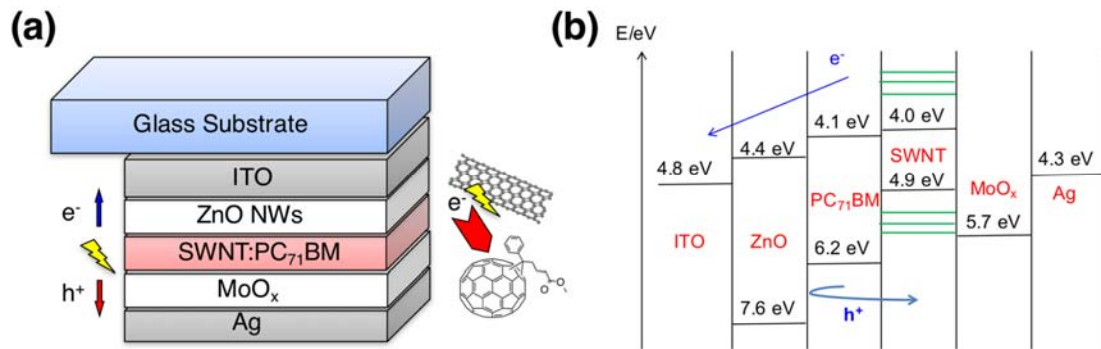


Figure 3. Illustration of a) an inverted solar cell where ZnO NW and SWNT:PC₇₁BM were used and b) the energy level diagram.

1.3 CNT as Charge Transporter and Others

Despite considerable research effort, the use of CNTs as a charge transporter did not yield in a substantial leap in PCE without the use of dopants and the introduction of inorganic materials, such as quantum dots (QDs). Kim and co-workers addressed the intrinsic limitation imposed by the recombination effect and improved PCE by more than 30% through B- and N-doping (Table 1: Report L).⁴⁶ B and N doped CNTs functioned as effective charge-selective transport materials without a quenching effect. The low work function of N-doped CNTs aligned well with the electron-transport energy level, while the high work function of B-doped CNTs aligned well with the hole transport level. Kamat and colleagues studied the interaction between SWNTs and light-harvesting CdS.^{47,48} Since then, Raffaele and colleagues⁴⁹ demonstrated the first incorporation of QDs into SWNT composites in 2005 and colloidal QD-decorated N-doped CNTs were developed for synergistic charge separation and transport enhancement. Positively charged QDs could directly attach at N-doped sites of CNTs via electrostatic interactions. Such an ideal hybrid structure without an adhesive layer showed a synergistic effect, combining effective electron and hole separation. Efficiency soared, reaching 4.7–6.11% (Table 1: Report M) when using indene-C60 bisadduct (ICBA) as the electron acceptor⁵⁰ and climbing to 7.5–8.6% upon further development using different organic photoactive materials (Table 1: Report N).⁵¹ With QDs as an acceptor and doped CNTs as an efficient charge transporter, these studies demonstrate that work function-tunable chemically

modified CNTs have the potential to improve charge separation, transport, and recombination in SWNT-based OSCs, which generally suffer from trapping and slow transport of charge carriers in their organic active layers and energy-level mismatch at interfaces.

Other approaches have been taken to apply SWNTs in the active layer. We reported the use of multilayered MoS₂ on low-cost metallic/semiconducting SWNTs as the electron acceptor in a bulk heterojunction with P3HT in inverted OSCs (Figure 4).⁵² MoS₂ is an inorganic material that is intrinsically immiscible with organic compounds. However, we were able to disperse it in organic matrix by exploiting the tendency of SWNTs to intercalate with P3HT through π - π interactions. The successful binding of MoS₂ onto SWNT bundles and its photovoltaic effect was clearly seen in PCE of 0.46% (Table 1: Report O).

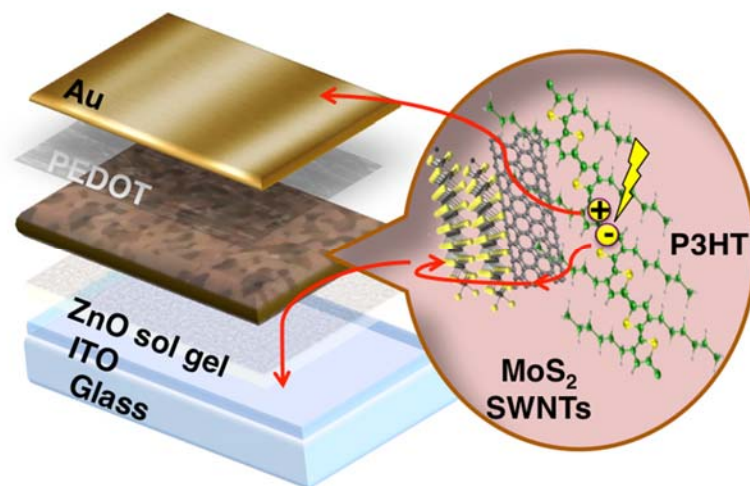


Figure 4. Illustration of MoS₂:SWNT:P3HT-based solar cells.

We have briefly reviewed the use of SWNTs as the light harvester or charge transporter in the photoactive layer of solar cells. Chirality, chemical doping, and dispersibility in solution were crucial factors in achieving high performance. Various approaches have been introduced to improve SWNT applications and these findings expanded the possibilities of CNT technology in solar cells. Yet, this is still just the tip of the iceberg. Uniform blending of the electron-donating conjugated polymer and the

electron-accepting CNT is one of the most challenging as well as crucial aspects in creating efficient photocurrent collection in CNT-based OSC devices. Therefore, research on using CNTs in the photoactive layer of OSC devices is still in the early stages and room remains for novel methods to take better advantage of the advantageous properties of CNTs.

Table 1. Photovoltaic data of representative devices from literature, in which SWNTs have been used as either a light-harvester or charge transporter.

	Structures	PCE (%)	Note
A	MWNT/PPV/Al	1.8	The very first OSC using CNTs in the active layer
B	ITO/P3OT:SWNT/Al	0.04	The first OSC using SWNTs in the active layer
C	ITO/PEDOT/P3HT:C ₆₀ -SWNT/Au	0.57	C ₆₀ -SWNT composites were used
D	ITO/PEDOT/CNT:P3HT:PCBM/LiF/Al	2.0	Studied the effect of CNT content in composites
E	ITO/PEDOT:SWNT/P3HT:PCBM/Al	4.9	Investigated positional effect of SWNTs on PCE
F	ITO/PEDOT/SWNT:P3HT/BCP/Al	0.72	Using semiconducting SWNTs coated with P3HT
G	ITO/SWNT:PCBM/C60/BCP/Ag	1.3	SWNTs as electron donor and infrared absorber
H	ITO/PEDOT/SWNT:r-GO:C ₇₀ /C ₇₀ /Al	0.85	Incorporated reduced graphene oxide
I	ITO/PEDOT/TFB/PC ₇₁ BM:r-GO:SWNT/Al	1.3	Further improved PCE by using PC ₇₁ BM
J	ITO/PEDOT/SWNT/C ₆₀ /Ag	0.46	No SWNT composite, attempt at full-carbon SC
K	ITO/ZnO NW/SWNT:PC ₇₁ BM/MoO _x /Ag	3.1	Application of ZnO NW
L	ITO/PEDOT/P3HT:PCBM:B-CNT/TiO _x /Al	4.1	B-, N-doped MWNTs were used to enhance PCE
M	ITO/PEDOT/P3HT:ICBA:QD:N-CNT/TiO _x /Al	6.1	QDs were used to enhance doping and dispersion
N	ITO/PEDOT/PTB7:PC ₇₁ BM:N-CNT/Ca/Al	8.6	Low band-gap polymer, PTB7 was used
O	ITO/ZnO/P3HT:SWNT/MoS ₂ /PEDOT/Au	0.46	SWNTs enabled a mixture of MoS ₂ and P3HT

2. Single-walled Carbon Nanotubes as a Transparent Electrode in Solar Cells

Many types of solar cells have been developed over the years: silicon solar cells, followed by OSCs^{53–55}, and most recently perovskite solar cells (PSCs), which have emerged as a focus of research. A critical aspect common to these devices is their transparent electrode through which light travels before causing excitation in the active layer. Conventionally, ITO has been used as the transparent electrode, and is an essential component in almost all the devices discussed in the first section. The high conductivity and transmittance of ITO are unparalleled thus far. There have been many attempts to replace ITO because of its high cost and limited earth-abundance. Other downsides include its brittleness, which makes it unable to withstand cyclic flexibility tests without breaking. One of the other drawbacks includes ITO's vulnerability to high temperature. Therefore, fluorine-doped tin oxide (FTO), which can withstand higher temperatures than ITO, is sometimes used instead. Avoiding these limitations by using alternative transparent electrode materials has therefore been the subject of intense research for many years.^{56,57} The difficulty has been the finding an alternative electrode that is not only robust and cheap, but also optically transparent and electrically conductive.^{58–60} CNTs have good optical transparency over a broad range from the visible to the near-infrared as well as high electrical conductivity.^{61–64} In addition to this, the outstanding mechanical resilience of CNTs not only exceeds that of ITO but also affords flexibility to solar cell devices. SWNTs are effective for hole collection because their work function is in the range 4.8 to 5.0 eV, which is higher than that of ITO (usually less than 4.8 eV).⁶⁴ The cost of CNT fabrication has also been reported to be the same or lower than that of ITO.⁶⁵ In this section, we discuss the feasibility of SWNTs as a transparent flexible electrode in solar cells by reviewing applications reported to date.

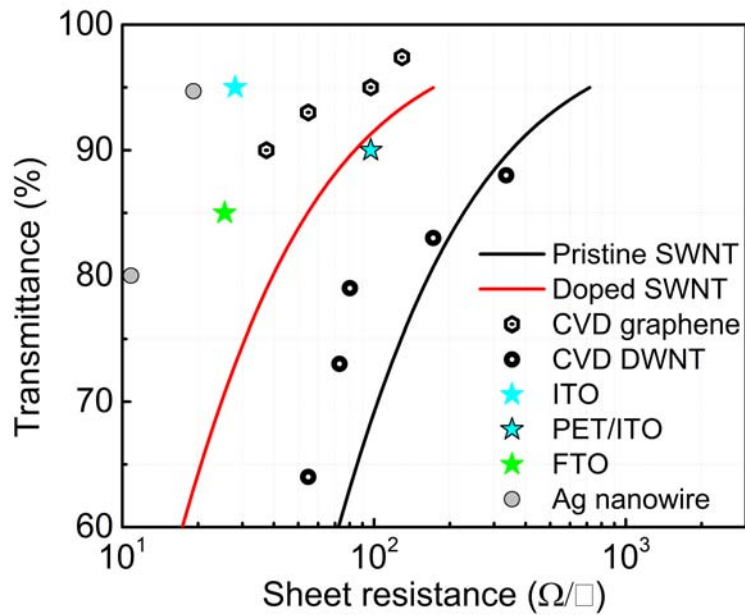


Figure 5. Sheet resistance vs. transmittance plot for various transparent conductors (Pristine SWNT [63], Doped SWNT [63], CVD graphene [69], CVD DWNT [70], ITO from Kuramoto Co., Ltd., PET/ITO from Nitto Denko Co., Ltd., FTO from Nippon Sheet Glass Co., Ltd., and Ag nanowires [67])

2.1 Single-walled Carbon Nanotubes as a Transparent Electrode in Silicon Solar Cells

The high cost of silicon led scientists to look for other semiconductors that were viable alternatives. It was found that CNTs can serve as both photogeneration sites and the charge transport layer. A semi-transparent CNT film next to an *n*-type crystalline silicon substrate creates high-density *p-n* heterojunctions inducing charge separation in which electrons are extracted through *n*-Si and holes are extracted through CNTs. Although the mechanism is not fully understood, there are two prevailing theories. In the first theory, the CNT film is the *p*-type semiconductor material (Figure 6a)⁷²⁻⁷⁴ and

silicon absorbs the photons dominantly as normal silicon solar cells.⁷⁵ Although CNT films can absorb photons, this is limited when the film is transparent to the incident light pass. The photons generate excitons, and then the excitons are separated into free charge carriers by the built-in potential between the *p*-type CNT and *n*-type Si. The second theory is that a Schottky junction is formed when metallic CNT is in contact with semiconductor Si, and typically it is believed that a thin insulator, SiO₂ exists (Figure 6b)^{76,77} again as normal silicon solar cells.^{78–79} Excitons are produced by silicon absorbing photons and diffuse into SiO₂ which is formed by the built-in potential of the Fermi level difference and minority carriers are transported by tunneling through the thin layer of SiO₂. Taking the chirality of CNTs into account can further complicate the mechanism. Many individual nanotubes are present in a device, and each forms a heterojunction with the *n*-type silicon. As CNTs exhibit semiconducting or metallic behavior depending on their chirality, a *p-n* junction can be expected for the former and a Schottky junction for the latter.

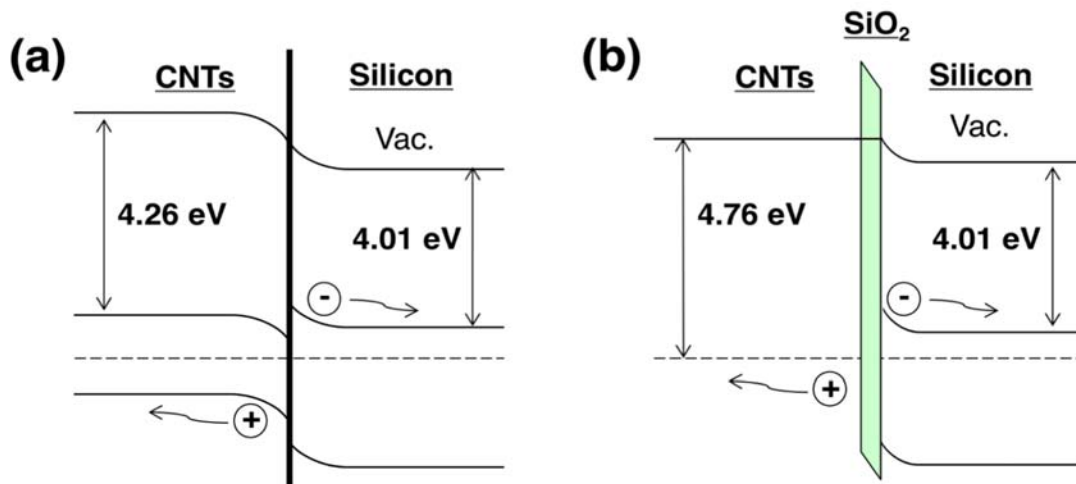


Figure 6. Illustration of a) the CNT film functioning as a *p*-type emitter material and b) a Schottky junction is formed by an insulator, SiO₂ (work functions taken from references 72, 77)

The very first CNT-based silicon solar cell was reported by Jia *et al.*, in which they used double-walled CNTs. The CNTs performed multiple functions, such as charge separation, charge transport, and charge collection.⁸⁰ On the same year, Biris and colleagues showed a PCE of 1.3% (Table 2: report A) using SWNT.⁸¹ They formed this SWNT film by spray coating from a dimethylformamide suspension. They also tested post-treatment with SOCl_2 for the first time, which led to mobility and carrier density being increased by more than 60% according to Hall effect measurements. In the following year, Biris and co-workers reported a PCE of 4.5% (Table 2: report B).⁸² Again, they used the same SOCl_2 treatment, but transferred as-grown SWNT onto silicon.⁸³ More detailed studies of acid doping were subsequently conducted. They identified SOCl_2 as a *p*-type dopant that shifts the Fermi level of SWNTs below ν_1 , thus increasing the mobility and carrier density (Figure 7a).⁸⁴ This results in suppression of the S_{11} transition in the semiconducting SWNTs and stronger doping would suppress the S_{22} transition as well (Figure 7b) as observed by near-infrared absorption spectroscopy. It is argued by some researchers that after the acid treatment, CNTs and silicon switched from acting as a *p-n* junction to acting as a Schottky junction, giving the CNTs more metallic character. In other words, the mechanism acting in the interface network changed from variable range hopping to tunneling. The correlation between suppression of the transitions and CNT chirality was analyzed in greater detail by Levitsky and colleagues (Table 2: report C).⁸⁵ They used the photocurrent with a high-resolution absorption spectrum to identify the S_{11} band at around 1100 nm, corresponding to the (7,6) and (8,6) chiralities of SWNTs. They also discovered that metallic SWNTs function as a light absorber in a Schottky junction, though their device showed a PCE of only 1.7%. In the same year, Rinzler and colleagues reported a whopping 10.9% (Table 2: Device D).⁸⁶ The devices initially had a PCE of 8.5%, but by using electrolyte junction control of gate potential, they controlled the Fermi level to strengthen the interface dipole at the electronic junction. Jia *et al.* further improved PCE by treating SWNTs with dilute nitric acid (Table 2: Device E).⁸⁷ The HNO_3 treatment increased FF greatly by reducing series resistance (R_s) as a result of *p*-doping lowering the Fermi level of the SWNTs. They also demonstrated improved doping in the effectiveness by employing porous CNTs. According to them, the contact between CNTs and silicon was significantly improved

through formation of a semiconductor/electrolyte interface by the exposed silicon surface in the empty areas without CNTs. They further demonstrated NaCl doping to show that any wet state of CNT doping works as an electrolyte bridge. Subsequently, encapsulating the active area with polydimethylsiloxane (PDMS) further improved PCE and stability (Table 2: Report F).⁸⁸ They discussed that the improvement in PCE came from the anti-reflective function of the PDMS film and SiO₂ layer increasing V_{oc} by reducing charge recombination. Stability was improved by the PDMS protecting *n*-Si from oxidation. In a follow-up study, Rinzler and colleagues achieved a PCE of 12% using grid lines of SWNTs etched to cover only a fraction of the silicon surface (Table 2: Report G).⁸⁹ The addition of electrolyte immediately improved the device performance. The mechanism at play is said to be similar to that of nitric acid doping, where improvement in performance came partly from the accumulation of NO₃⁻ at the junction, which has electron-blocking functionality in addition to that of SiO₂. Likewise, the surface dipole of the accumulated negative ions in the electrolyte is supposed to block electrons, preventing charge recombination.⁹⁰ Matsuda and colleagues reported 2.4% PCE by optimizing the thickness of (6,5) SWNTs (Table 2: Report H).⁹¹ Returning to acid doping, an even higher PCE of greater than 11.2% was achieved by Taylor and colleagues via keeping the acid inside the void space of CNTs (Table 2: Report I).⁷³ They discussed the characteristics of dark forward current density with varying temperature and found that temperature-dependent current rectification originates from thermally activated band-to-band transitions of carriers in silicon and that the SWNT thin films established a built-in potential for carrier separation/collection. In the same year, Taylor published another paper with a marginally improved PCE of 11.5%. a new super acid slide casting method was used for the CNT fabrication (Table 2: Report J).⁹² 10.0% PCE was also achieved by us using micro honeycomb CNT network in silicon SCs (Table 2: Report K).⁹³ We reported vertically aligned SWNTs and treated with water to form honeycomb network on *n*-Si substrate. CNTs and graphene were combined with crystalline silicon wafers to fabricate silicon solar cells. Solar cells with direct graphene-to-silicon contact exhibited better characteristics than did those with CNT-to-silicon contact, owing to improved junction quality and increased contact area. Using the composite films, the obtained SWNT/graphene/Si solar cells reached a PCE of 14.9% (Table 2: Report L).⁹⁴ A problem

with wet acid doping is a high exciton quenching rate, but they resolved this issue by employing aligned CNTs, which shortened the transport distance. Moreover, the aligned CNTs were in better contact with the silicon as evident from an increase in J_{sc} . Cui *et al.*, used pristine aerosol SWNTs with long bundle lengths to fabricate SWNT/Si solar cells.⁹⁵ A PCE approaching 11% was achieved using a pristine SWNT without any chemical treatment (Table 2: Report M). More importantly, the solar cells were stable for at least 10 months in air without any passivation. In fact, a slight increase in PCE after storing in air, in contrast to previous results in the literature. Li *et al.*,⁹⁶ demonstrated an *n*-SWNT/*p*-Si photovoltaic system by tuning SWNTs from *p*-type to *n*-type through polyethylene imine functionalization. Recently, Matsuda and colleagues used metal oxide layers to prepare both *p*-SWNT/*n*-Si and *n*-SWNT/*p*-Si with significantly improved PCEs.⁹⁷ The metal oxides also serve as both an antireflective layer and an efficient carrier dopant, leading to reduced loss of incident solar light and increased photocurrent, respectively. As a consequence, the photovoltaic performance of both *p*-SWNT/*n*-Si and *n*-SWNT/*p*-Si heterojunction solar cells using MoO_x and ZnO layers was improved, resulting in very high PCEs of 17.0% and 4.0%, respectively (Table 2: Report N).

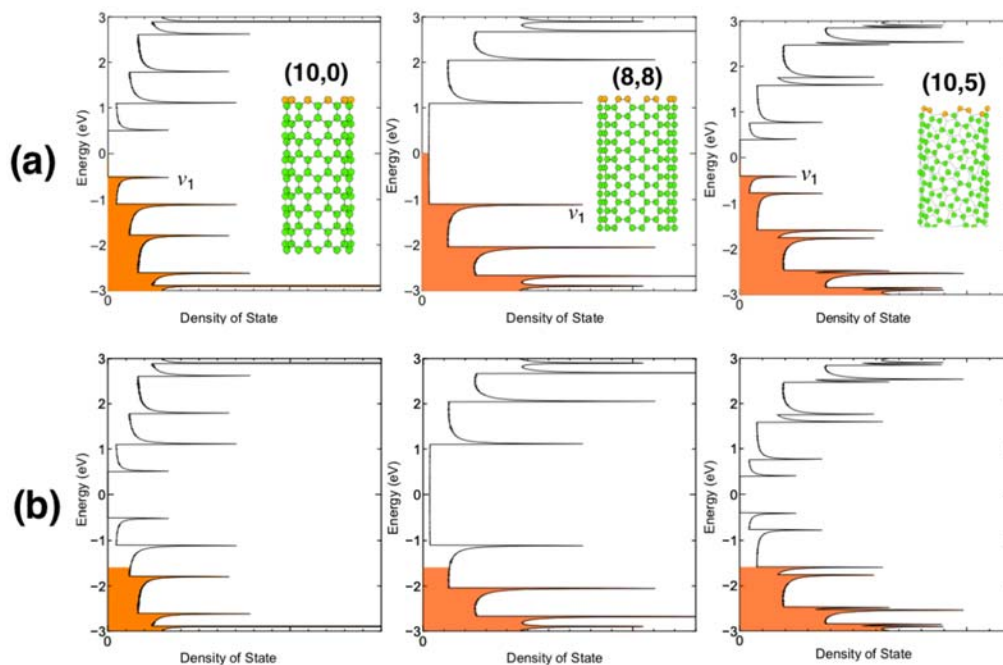


Figure 7. a) Density of states and v_1 of an armchair SWNT, a zig-zag SWNT, and a chiral SWNT. b) Density of states after *p*-doping.

Table 2. Photovoltaic data of representative SWNT-used silicon solar cells from literature.

	CNT treatment	Si treatment	Structures	PCE (%)	Note
A	SOCl ₂	n/a	Si/SWNT	1.3	The first SWNT-based silicon solar cells
B	SOCl ₂	n/a	Ag/Si/SWNT/Ag	4.5	Transferring as-grown SWNT onto silicon
C	n/a	HF	Ag/Si/SWNT/Cr/Au	1.7	Studied CNT chirality and transition reduction
D	n/a	oxide etch	-	10.9	Electrolyte junction control of gate potential
E	HNO ₃ /NaCl	HF	Ti/Si/SWNT/Au	13.8	<i>p</i> -doping of HNO ₃
F	HNO ₃	HF	Ti/Si/SWNT/Au	10.0	Encapsulating the active area by PDMS
G	n/a	oxide etch	-	12.0	Grid lines of SWNTs to cover small area of Si
H	-	-	-	2.4	(6,5) SWNTs with optimized thickness
I	HNO ₃	HF	Al/Si/SiO ₂ /SWNT/Cr/Au	11.3	Keeping acid inside the void space of CNTs
J	HNO ₃	HF	Au/Si/SiO ₂ /SWNT/Cr/Au(Al)	11.5	super acid slide casting method
K	HNO ₃	-	Pt/Ti/n-Si/SWNT/Pt	10.0	Micro honeycomb network CNTs
L	-	-	-	14.9	SWNTs and graphene comparison next to Si
M	-	-	Pt/Ti/n-Si/SWNT/Pt	11	Application aerosol SWNTs
N	MoO _x	HF	In/Si/SWNT/MoO _x /Au	17.0	Application of MoO _x doping.

Since the early reports of around 1%, CNT-Si solar cells have seen rapid performance gains up to around 17%. However, the mechanism is still not clear, as the Schottky metal oxide junction theory established by Jia *et al.* contradicts with the *p-n* junction theory of Ong *et al.*⁸⁵ However, the Schottky metal oxide junction theory seems to be more dominant for the time being. Although the polychirality of CNTs further obscures this issue, pure CNTs are becoming increasingly available, so we can anticipate a clearer understanding in the near future. Considering the decades of wide-ranging research into silicon solar cells, this is still a relatively small area of research and it is worthwhile to investigate these devices further. The apparent ease with which high PCEs have been rapidly achieved by a limited number of research groups, is both exciting and sure to prompt further research.

2.2 Single-walled Carbon Nanotubes as a Transparent Electrode in Organic Solar Cells

OSCs received spotlight in recent academic research.^{98–100} OSCs provide flexibility and low cost that silicon solar cells cannot match. OSCs utilize conductive organic compounds as electron donors and electron-rich fullerene derivatives as electron acceptors.^{55,101} Owing to their high absorption coefficient, low cost and mechanical flexibility, OSCs have established as one of the important categories of the solar cell research. Nevertheless, despite laudable achievements in recent years, OSCs are still faced with limitations including the fixed light absorption range of organic compounds, restricted hole mobility, and intrinsic instability.¹⁰² Above all, the maximum PCEs of OSCs (*ca.* 10%) are lagging behind those of silicon solar cells (*ca.* 20%).

Early on, many studies were conducted that used CNTs as a light harvester in OSCs, as discussed in the first section of this chapter.²¹ Nowadays, however, CNTs in OSCs are typically not responsible for exciton generation upon light absorption. Instead, a more promising approach is to use CNTs on either side of the device as a charge-collecting transparent electrode. In this section, we focus mainly on the use of SWNTs as electrodes in OSCs. SWNTs have been used mostly as the anode. For example, Gruner and colleagues reported the use of SWNTs as a transparent anode and demonstrated efficient, flexible OSCs with a structure of polyethylene terephthalate (PET)/SWNT/poly(3,4-ethylenedioxythiophene) (PEDOT)/P3HT:PCBM/Al. SWNTs were deposited using a filtration method, and PEDOT was used to coat the rough CNT surface and lower R_s through its acidic nature functioning a weak dopant (Table 3: Report A).¹⁰³ The resulting flexible device showed a PCE of 2.5%, which was close to that of the ITO glass-based control device. Moreover, PET-based devices demonstrated outstanding flexibility, with good performance even at large bending angles, where the ITO-based devices cracked at a bending angle of 60°. ¹⁰⁴ In another study, SWNTs were used as a transparent cathode, which requires a lower Fermi level (Table 3: Report B).¹⁰⁵ Chhowalla and co-workers fabricated inverted OSCs with a configuration of PET/SWNT/ZnO nanowire/P3HT/Au, which achieved a maximum PCE of 0.6%. The resulting OSCs showed good long-term stability, but the PCE was extremely low presumably because of an intrinsic energy-level mismatch and a lack of doping effect. Thus, researchers have focused on applying SWNTs, Franghiadakis and colleagues reported hybridization of PEDOT and SWNTs to replace both ITO and PEDOT as a hole-

transporting electrode (Table 3: Report C).¹⁰⁶ A PCE of 1.3% was achieved and the only drawback was low FF (0.4), which arose from high resistance between the polymer and SWNT film. Four years later, DeMello and colleagues investigated two SWNT film fabrication methods: spin-coating from dichloroethane solvent and spray coating from deionized water containing sodium dodecyl sulfate or sodium dodecyl benzene sulfonate as a surfactant (Table 3: Report D).¹⁰⁷ Films produced by both of the methods were mechanically robust. HNO₃-treated SWNT films yielded sheet resistances of around 100 Ω sq⁻¹ with an average transmittance of 90%. Spin-coated SWNT films provided better performance and a PCE of 2.3%. In the following year, Hersam and colleagues focused on reducing the roughness of SWNTs in order to increase performance via improved morphology (Table 3: Report E).¹⁰⁸ In addition, they investigated the change in PCE according to the ratio of metallic and semiconducting SWNTs, and found that a purely metallic (99.9% metallic) SWNT film gave the best performance as the transparent electrode. The device using a purely metallic SWNT film exhibited a PCE of 2.035%, in stark contrast to the value of 0.038% for the device using a purely semiconducting SWNT film. Zarbin and colleagues used interfacial synthesis of CNTs to produce a transparent conductive film for ITO-free OSCs (Table 3: Report F).¹⁰⁹ The interfacial synthesis produced a mixture of SWNTs and MWNTs and very high CNT loadings could be achieved using these films without a significant effect on transparency. Secondary polyaniline was used for doping to achieve a PCE of 2.27% in a flexible device. The PCE of SWNT-based OSCs reached a new peak of 6.04% in 2015, when our laboratory reported OSCs based on aerosol-synthesized SWNTs (Table 3: Report G) (Figure 8 and 9).¹¹⁰ Anaerobic thermal annealing of CNTs next to MoO₃ increased their conductivity greatly.¹¹¹ This doping effect lasted much longer than that of HNO₃.¹¹² Using this approach, we thermally annealed an SWNT film sandwiched between MoO₃ layers at around 300 °C in nitrogen for longer than 2 hours. The composition of MoO₃ changed to MoO_x where x is between 2 and 3 (Figure 10).¹¹³ The same SWNT films were used as the top electrode in an inverted structure, which was reported in Scientific Reports.¹¹⁴ These semi-transparent OSCs with a top electrode consisting of laminated transparent SWNTs are highly promising when used in tandem or power-generating windows (Table 3: Report H) (Figure 11).

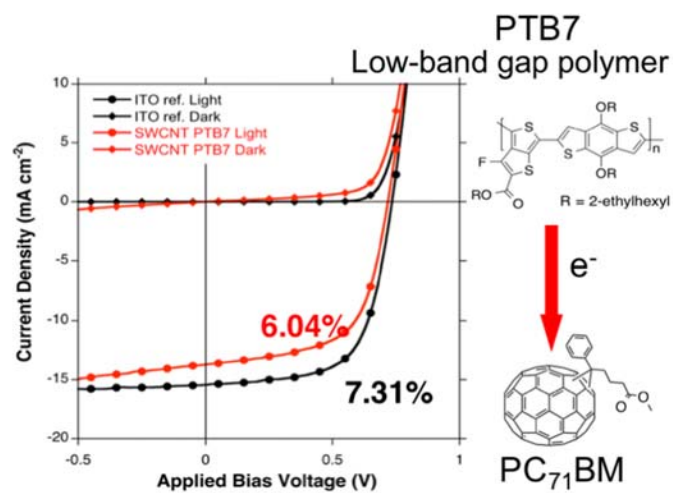


Figure 8. Current density–voltage curves of the devices from the report G.

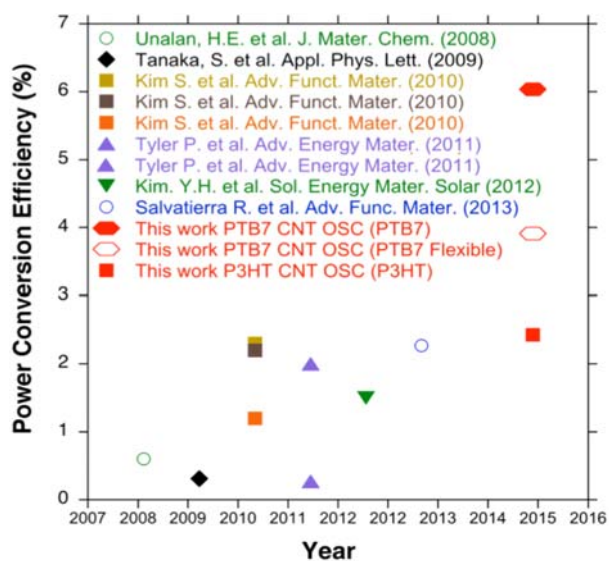


Figure 9. Literature PCE values of SWNT-based OSCs as compared to the work presented in reference 110.

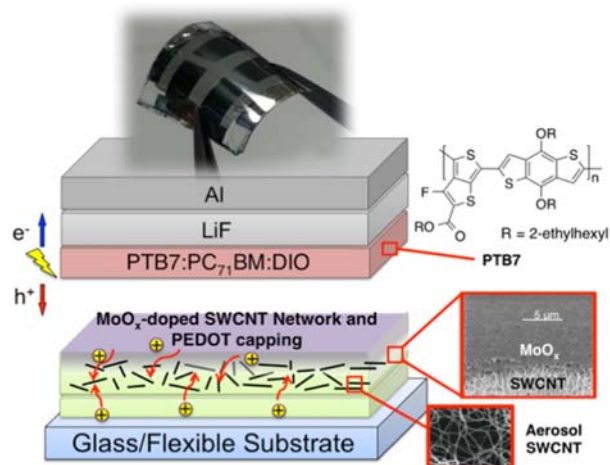


Figure 10. Schematic of the device from the report G.

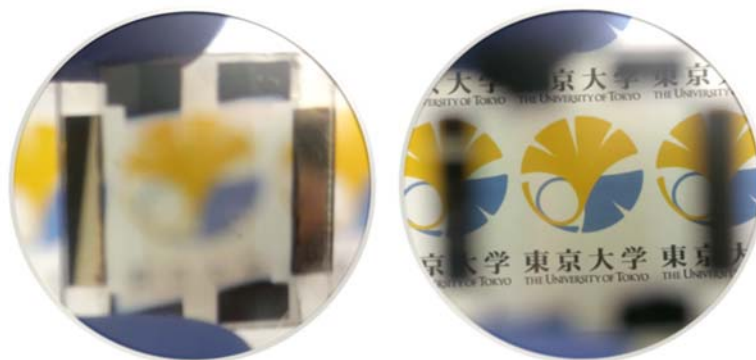


Figure 11. Transparent OSCs for window application.

From the results discussed above, we can see that SWNTs have shown tremendous potential for use in OSCs. They can replace not only ITO but also metal electrodes. Nevertheless, further study is needed, as these results do not completely stack up to the performance of ITO. We will discuss how to go about addressing this issue at the conclusion of this chapter.

Table 3. Photovoltaic data of representative SWNT-OSCs from literature.

	Structures	PCE (%)	Note
A	SWNT/PEDOT/P3HT:PCBM/Al	2.5	Filtration-transferred CNTs as anode on PET
B	PET/SWNT/ZnO NW/P3HT/Au	0.6	Filtration-transferred SWNTs as cathode on PET
C	SWNT/PEDOT/P3HT:PCBM/LiF/Al	2.3	Spin-coated SWNTs as anode
D	PEDOT-SWNTs/P3HT:PCBM/Al	1.3	SWNTs and PEDOT hybrid as anode

E	SWNT/PEDOT/P3HT:PCBM/LiF/Al	2.0	Purely metallic SWNTs as anode
F	CNT/PEDOT/F8T2/C ₆₀ /Al	2.27	CNT was generated by interfacial synthesis
G	MoO _x /SWNT/MoO _x /PEDOT/PTB7:PC ₇₁ BM/LiF/Al	6.04	Aerosol synthesized SWNT film
H	ITO/ZnO/PTB7/PTB7:PC ₇₁ BM/MoO ₃ /SWNT	4.1	p-doped SWNT film as top electrode

2.3 Single-walled Carbon Nanotubes as a Transparent Electrode in Perovskite Solar Cells

2.3.1 DSSCs

To discuss PSCs, let us first review dye-sensitized solar cells (DSSCs). Due to their simple fabrication and high efficiency, DSSCs have attracted considerable interest from researchers around the world. Titanium dioxide nanoparticles have been widely used as the working electrode in DSSCs because they provide higher efficiency and more robustness than any other metal oxide semiconductor investigated.¹¹⁵

To search for an effective counter electrode in DSSCs, Yanagida and co-workers examined different kinds of carbon materials.¹¹⁶ A PCE of 4.5% was obtained when SWNTs were used (Table 4: Report A). This value was comparable to that of platinum-sputtered fluorine-doped tin oxide-based DSSCs. There had been several attempts at fabricating DSSCs using a carbon material as the counter electrode, but this work was the first to produce a fair PCE.¹¹⁷ Later, Kim and colleagues investigated the effects of acid-treatment of SWNTs in a TiO₂ film with the dyes anchored. Compared with an unmodified cell, DSSCs using acid-treated SWNTs at the TiO₂/electrolyte interface had significantly improved photocurrent-voltage characteristics.¹¹⁸ The modified cell showed a 25% increase in J_{SC} , which resulted from improved contact between the acid-treated SWNTs and the TiO₂ particles and enhanced light scattering by TiO₂ clusters. For dye-linked, acid-treated SWNTs anchored to the TiO₂/electrolyte interface, V_{OC} increased by around 0.1 V, mainly due to the basicity of the TiO₂ surface from the NH groups of

ethylenediamine moieties in the anchored dye linked to the SWNTs. Kamat and co-workers reported a use of SWNTs not only as an electrode but also as a charge transporter.¹¹⁹ SWNTs utilized as conducting scaffolds in TiO₂-based DSSCs boosted PCE by a factor of 2 (Table 4: Report B). Titanium dioxide nanoparticles were scattered on an SWNT film to improve photo-induced charge separation and transport of carriers to the collecting electrode surface. An approximately 100 mV shift in the Fermi level of the SWNTs-TiO₂ system compared with the pristine TiO₂ indicated equilibration of the Fermi level between the two systems. The interplay between the TiO₂ and SWNTs for achieving charge equilibrium was an important factor in improving solar cell performance. Yoo and colleagues used the sol-gel method to prepare TiO₂-coated MWNTs for use a DSSC electrode (Table 4: Report C).¹²⁰ CNTs coated with TiO₂ achieved better solar cell performance through a reduction in R_s . Compared with the conventional device, the TiO₂-CNT (0.1 wt.%) cell showed a \square 50% increase in PCE from 3.32% to 4.97%, which is attributed to the increase in J_{sc} due to improved interconnectivity between the TiO₂ particles and the TiO₂-CNTs in the porous TiO₂ film.

2.3.2 PSCs

The emergence of organic-inorganic halide PSCs, which have PCEs of approximately 20%, has caused a paradigm shift from DSSCs to PSCs (Figure 12).^{121,122} Just within the five years that PSCs have been at the forefront of photovoltaics research. This entailed some of the researchers from OSC field to join the PSC research. Initially there was a confusion in coinage of the PSC structural types as to which is “normal” and which is “inverted”. A broad range of fabrication approaches and device concepts are being constantly developed and this diversity suggests that performance is still far from being fully optimized.¹²³

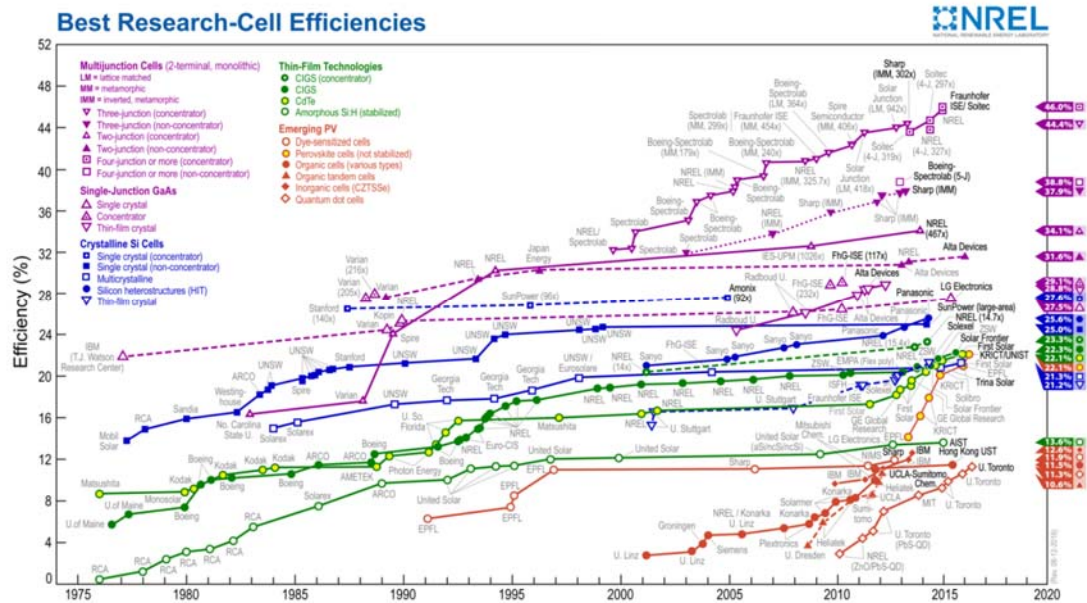


Figure 12. Certified solar cell PCE charts of all types of solar cells. We can see the PCEs of PSCs in orange (<https://www.nrel.gov/pv>).

The first application of an SWNT film as an ITO replacement in PSCs was demonstrated by our laboratory in 2015.¹²⁴ Specifically, we examined the use of SWNTs subjected to acid treatment, wettability control, and MoO_x doping. Diverse methods were employed to overcome the hydrophobicity of SWNTs and doping issues in solar cell devices, including modification of the wettability of PEDOT, MoO₃ thermal doping, and HNO₃ (aq) doping with various dilutions from 15% to 70 % (v/v) to minimize the instability and toxicity of the SWNTs. We discovered that isopropanol-modified PEDOT worked better than surfactant-modified PEDOT as an electron-blocking layer on SWNTs in PSCs because of superior wettability, whereas MoO₃ was incompatible due to energy-level mismatch. A diluted HNO₃ (35% v/v)-doped SWNT-based device produced the highest PCE of 6.32% among the SWNT-based PSCs tested—70% of the PCE of an ITO-based device (9.05%). Furthermore, a flexible cell was prepared using a PET film and realized a PCE of 5.38% (Table 4: Report D) (Figure 13). By inverting the structure, the SWNT film could be deposited from above to replace the metal electrode. Mhaisalkar

and co-workers reported transparent PSCs made by laminating aerosol-synthesized SWNT films onto a $\text{CH}_3\text{NH}_3\text{PbI}_3$ layer, with the SWNT films functioning as both a hole collector and electrode.¹²⁵ This enabled metal deposition, an energy-consuming vacuum process, to be bypassed. In the absence of an organic hole-transporting material and metal contact, $\text{CH}_3\text{NH}_3\text{PbI}_3$ and CNTs formed a solar cell with efficiency of up to 6.87% (Table 4: Report E). The $\text{CH}_3\text{NH}_3\text{PbI}_3/\text{CNTs}$ solar cells were semi-transparent and produced photovoltaic output under dual side illumination because of the transparency of the CNT electrode. Interfacial charge transfer in solar cells were investigated through photoluminescence and impedance measurements. The flexible and transparent CNT network film showed great potential for realizing flexible and semitransparent PSCs. With the addition of 2,2,7,7-tetrakis(N,N-di-p-methoxyphenylamine)-9,9,0-spirobifluorene (spiro-MeOTAD) to the CNT network, PCE improved from 6.87% to 9.90% as a result of enhanced hole extraction and reduced charge recombination. A similar approach was demonstrated by Wong and colleagues.¹²⁶ Ti foil- TiO_2 nanotubes with an organic-inorganic halide perovskite absorber and transparent CNTs was adopted in PSC fabrication. Ti foil- TiO_2 nanotubes were formed by one-step anodization. The composition served as a deposition scaffold and electron conductor for the perovskite absorber. Later, a transparent conductive CNT film was laminated on top of perovskite and served as a hole transporter as well as a transparent electrode for light illumination. A PCE of 8.31% was achieved, which is the highest among TiO_2 nanotube-based flexible solar cells. These kinds of PSCs, in which CNTs were used to replace the top metal electrode, reached their current peak in a study by Boschloo and co-workers.¹²⁷ They demonstrated highly efficient PSCs with a hybrid hole-transporting counter electrode based on aerosol-synthesized SWNT films and drop-cast spiro-MeOTAD. An average PCE of 13.6% with a maximum of 15.5% was recorded, while the reference solar cell with spiro-MeOTAD and a gold electrode showed an average of 17.7% (Table 4: Report F). The results revealed the feasibility of high-efficiency PSCs with carbon-based hole-transporting materials. The SWNTs function not only as a charge conductor or transporter, but also as an encapsulating layer that protects the device from water infiltration. The stability of PSCs using SWNTs was addressed by Snaith and colleagues (Table 4: Report G).¹²⁸ They demonstrated a method for mitigating thermal degradation

by replacing the organic hole-transporting material with polymer-functionalized SWNTs as in an insulating polymer matrix. With this sort of composite structure, a PCE of 15.3% was accomplished, along with strong retardation of thermal degradation and good resistance to water infiltration. Going back to the bottom transparent electrode, our group compared SWNT with graphene in the viewpoint of photovoltaic and mechanical performance (Table 4: Report H).¹²⁹ With the demonstration of 12.8% PCE, we discovered that using graphene electrode as the bottom electrode results in slightly higher photovoltaic performance than that of SWNT, yet SWNT had the upper hand in terms of mechanical resilience and reproducibility. The use of SWNT electrode expanded to replacing both metal and transparent metal oxide conductor. As shown in Fig. 14, flexible PSC using SWNT both as cathode and as anode is recently demonstrated by our group.¹³⁰ Although the achieved efficiency was 7.32%, a possibility of roll-to-product processability was demonstrated.

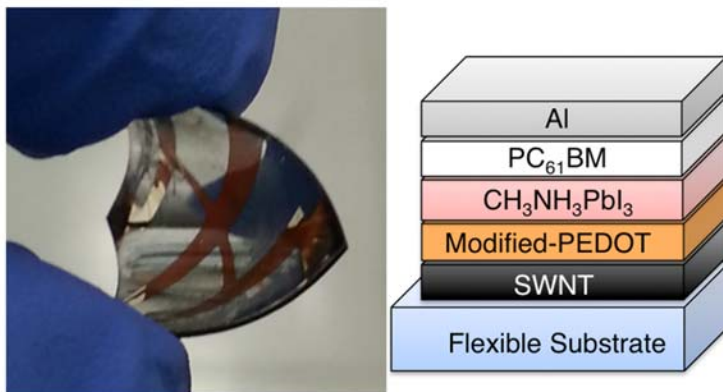


Figure 13. Flexible SWNT-PSC structure (right) and its picture (left).

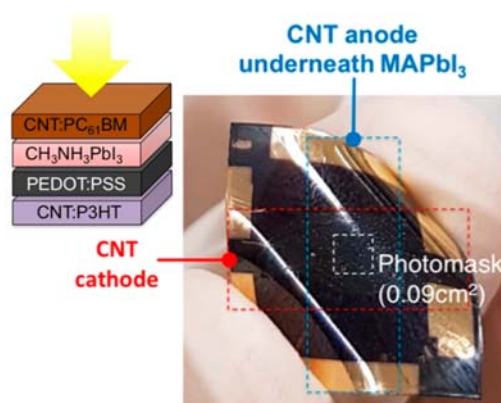


Figure 14. Flexible PSC using SWNTs both as cathode and as anode. structure (left) and its picture (right). (Table 4: Report J)

Table 4. Photovoltaic data of representative SWNT-DSSCs and -PSCs from literature.

	Structure or research impact	PCE (%)
A	membrane filter/SWNT/electrolyte/reflection layer/TiO ₂ /dye/FTO	4.5
B	TiO ₂ particles were scattered on SWNTs to improve charge separation and transport	0.6
C	DSSCs using the sol-gel method to obtain TiO ₂ coated MWNTs	4.97
D	SWNT/PEDOT/CH ₃ NH ₃ PbI ₃ /PCBM/Al	6.32
E	FTO/TiO ₂ /mesoporous TiO ₂ /CH ₃ NH ₃ PbI ₃ /SWNT/spiro-MeOTAD	9.90
F	FTO/TiO ₂ /mesoporous TiO ₂ /((FAPbI ₃) _{3-x} (MAPbBr ₃) _x)/SWNT/spiro-MeOTAD	15.5
G	FTO/TiO ₂ /Al ₂ O ₃ /CH ₃ NH ₃ PbI _x Cl _{3-x} /P3HT/SWNT/PMMA/Ag	15.3
H	SWNT/MoO ₃ /PEDOT/CH ₃ NH ₃ PbI ₃ /C ₆₀ /BCP/Al	12.8
J	SWNT/P3HT/CH ₃ NH ₃ PbI ₃ /PCBM/SWNT	7.32

Up to this point, we have looked at the applications of SWNTs as transparent electrodes in solar cells. There is no doubt that the excellent properties of SWNTs make them promising candidates for incorporation into future low-cost, multifunctional photovoltaic devices. Their application initially started as the photoactive materials in solar cells due to their semi-conducting properties. However, difficulties in purification slowed the progress. In silicon solar cells, SWNTs began to be used as both electrode and

photoactive materials, boosting their potential as a solar cell component. With the emergence of thin film solar cells, namely OSCs and PSCs, the number of reports on application of SWNTs soared up rapidly as they could replace ITO, generating flexible and low-cost photovoltaics. There has been intermittent reports on their usage as the photovoltaic materials, again the progress was limited by challenging nature of the separation of the semiconducting SWNTs. Overall, many challenges still remain. Below, we outline five key points that are crucial for further improvement:

1. Conductivity and transparency: The performance of photovoltaic devices is strongly dependent on CNT properties. The sheet resistance and transparency of CNTs are not yet comparable to those of ITO, which has sheet resistance of around $5 \Omega \text{ sq}^{-1}$ and transparency of more than 90%. Therefore, it is imperative that more stable and effective dopants be investigated.

2. Fermi level: To achieve high performance, especially as the cathode in OSCs, CNT electrodes must have a proper Fermi level to minimize energy barriers for charge transfer. Normally, carbon materials have a Fermi level of 4.5–5 eV, similar to that of an ITO film with a work function of 4.6–4.8 eV. The Fermi level can be tuned for various electrode uses.^{128–131} Materials like PEDOT are commonly used to increase the Fermi level for charge injection at the anode, whereas materials like Cs_2CO_3 are used to reduce the Fermi level for electron collection at the cathode.

3. Wettability: CNTs are hydrophobic, so either they need to be made hydrophilic or materials being deposited on top need to be hydrophobic. Even better would be deposition of the material by a method that is independent of the wettability, such as thermal evaporation. Many chemical treatments to increase hydrophilicity decrease conductivity by introducing oxygen-containing groups or defects. Thus, other methods are needed that do not undermine the properties of CNTs while improving the wettability.

4. Surface roughness: A rough surface of CNTs creates a shunt pathway within the device, which results in reduced performance. The reproducibility of SWNT-based OSCs mainly hinges on their surface roughness. Therefore, much more attention should

be paid to keeping the surface smooth and clean during the fabrication and processing of SWCNTs.

5. Encapsulation: Device stability under ambient conditions is a crucial issue for practical applications, especially for OSCs and PSCs. The photoactive materials of these types of cells are rather unstable in air, and the barrier properties of plastic encapsulation are simply not good enough. Therefore, it is necessary to develop a flexible barrier that can passivate the device effectively. CNTs have shown some promise in this regard, yet not much research has been conducted. Further study will help open a path to more industrially viable CNT-based solar cells.

References

- (1) Avouris, P.; Freitag, M.; Perebeinos, V. Carbon-Nanotube Photonics and Optoelectronics. *Nat. Photonics* **2008**, *2* (6), 341–350.
- (2) O'Connell, M. J.; Bachilo, S. M.; Huffman, C. B.; Moore, V. C.; Strano, M. S.; Haroz, E. H.; Rialon, K. L.; Boul, P. J.; Noon, W. H.; Kittrell, C.; Ma, J.; Hauge, R. H.; Weisman, R. B.; Smalley, R. E. Band Gap Fluorescence from Individual Single-Walled Carbon Nanotubes. *Science* **2002**, *297* (5581), 593-596.
- (3) Lebedkin, S.; Hennrich, F.; Kiowski, O.; Kappes, M. M. Photophysics of Carbon Nanotubes in Organic Polymer-Toluene Dispersions: Emission and Excitation Satellites and Relaxation Pathways. *Phys. Rev. B - Condens. Matter Mater. Phys.* **2008**, *77* (16), 165429.
- (4) Kataura, H.; Kumazawa, Y.; Maniwa, Y.; Umez, I.; Suzuki, S.; Ohtsuka, Y.; Achiba, Y. Optical Properties of Single-Wall Carbon Nanotubes. *Synth. Met.* **1999**, *103* (1-3), 2555–2558.
- (5) Berson, S.; de Bettignies, R.; Bailly, S.; Guillerez, S.; Jousset, B. Elaboration of P3HT/CNT/PCBM Composites for Organic Photovoltaic Cells. *Adv. Funct. Mater.* **2007**, *17* (16), 3363–3370.
- (6) Chaudhary, S.; Lu, H.; Müller, A. M.; Bardeen, C. J.; Ozkan, M. Hierarchical Placement and Associated Optoelectronic Impact of Carbon Nanotubes in Polymer-Fullerene Solar Cells. *Nano Lett.* **2007**, *7* (7), 1973–1979.
- (7) Ma, B. H.; Yip, H.; Huang, F.; Jen, A. K.-Y.; Ma, H.; Yip, H.; Huang, F.; Jen, A.

- K.-Y. Interface Engineering for Organic Electronics. *Adv. Funct. Mater.* **2010**, *20* (9), 1371–1388.
- (8) Steim, R.; Kogler, F. R.; Brabec, C. J. Interface Materials for Organic Solar Cells. *J. Mater. Chem.* **2010**, *20* (13), 2499–2512.
- (9) Li, G.; Shrotriya, V.; Huang, J.; Yao, Y.; Moriarty, T.; Emery, K.; Yang, Y. High-Efficiency Solution Processable Polymer Photovoltaic Cells by Self-Organization of Polymer Blends. *Nat. Mater.* **2005**, *4* (11), 864–868.
- (10) Park, S. H.; Roy, A.; Beaupré, S.; Cho, S.; Coates, N.; Moon, J. S.; Moses, D.; Leclerc, M.; Lee, K.; Heeger, A. J. Bulk Heterojunction Solar Cells with Internal Quantum Efficiency Approaching 100%. *Nat. Photonics* **2009**, *3* (5), 297–302.
- (11) Huynh, W. U. Hybrid Nanorod-Polymer Solar Cells. *Science* **2002**, *295* (5564), 2425–2427.
- (12) Lee, J. U. Photovoltaic Effect in Ideal Carbon Nanotube Diodes. *Appl. Phys. Lett.* **2005**, *87* (7), 073101.
- (13) Avouris, P.; Freitag, M.; Perebeinos, V. Carbon-nanotube photonics and optoelectronics. *Nat. Photon.* **2008**, *2* (6), 341-350.
- (14) Fuhrer, M. S. Crossed Nanotube Junctions. *Science* **2000**, *288* (5465), 494–497.
- (15) Yang, F.; Wang, X.; Zhang, D.; Yang, J.; Luo, D.; Xu, Z.; Wei, J.; Wang, J.-Q.; Xu, Z.; Peng, F.; Li, X.; Li, R.; Li, Y.; Li, M.; Bai, X.; Ding, F.; Li, Y. Chirality-specific growth of single-walled carbon nanotubes on solid alloy catalysts. *Nature* **2014**, *510* (7506), 522-524.
- (16) Yuan, Y.; Karahan, H. E.; Yıldırım, C.; Wei, L.; Birer, Ö.; Zhai, S.; Laua, R.; Chen, Y. “Smart poisoning” of Co/SiO₂ catalysts by sulfidation for chirality-selective synthesis of (9,8) single-walled carbon nanotubes. *Nanoscale*, **2016**, *8*, 17705-17713.
- (17) Arnold, M. S.; Stupp, S. I.; Hersam, M. C. Enrichment of Single-Walled Carbon Nanotubes by Diameter in Density Gradients. *Nano Lett.* **2005**, *5* (4), 713–718.
- (18) Arnold, M. S.; Green, A. a; Hulvat, J. F.; Stupp, S. I.; Hersam, M. C. Sorting Carbon Nanotubes by Electronic Structure Using Density Differentiation. *Nat. Nanotechnol.* **2006**, *1* (1), 60–65.
- (19) Liu, H.; Nishide, D.; Tanaka, T.; Kataura, H. Large-scale single-chirality separation of single-wall carbon nanotubes by simple gel chromatography. *Nature Commun.* **2011**, *2*, 309.

- (20) Fagan, J. A.; Khripin, C. Y.; Silvera Batista, C. A.; Simpson, J. R.; Háro, E. H.; Hight Walker, A. R.; Zheng, M. Isolation of Specific Small-Diameter Single-Wall Carbon Nanotube Species via Aqueous Two-Phase Extraction. *Adv. Mater.* **2014**, *26* (18), 2800–2804.
- (21) Kymakis, E.; Alexandrou, I.; Amaratunga, G. A. J. High Open-Circuit Voltage Photovoltaic Devices from Carbon-Nanotube-Polymer Composites. *J. Appl. Phys.* **2003**, *93* (3), 1764.
- (22) Landi, B. J.; Raffaele, R. P.; Castro, S. L.; Bailey, S. G. Single-Wall Carbon Nanotube-Polymer Solar Cells. *Prog. Photovoltaics Res. Appl.* **2005**, *13* (2), 165–172.
- (23) Kazaoui, S.; Minami, N.; Nalini, B.; Kim, Y.; Hara, K. Near-Infrared Photoconductive and Photovoltaic Devices Using Single-Wall Carbon Nanotubes in Conductive Polymer Films. *J. Appl. Phys.* **2005**, *98* (8), 084314.
- (24) Ago, H.; Petritsch, K.; Shaffer, M. S. P.; Windle, A. H.; Friend, R. H. Composites of Carbon Nanotubes and Conjugated Polymers for Photovoltaic Devices. *Adv. Mater.* **1999**, *11* (15), 1281–1285.
- (25) Kymakis, E.; Amaratunga, G. A. J. Single-Wall Carbon Nanotube/conjugated Polymer Photovoltaic Devices. *Appl. Phys. Lett.* **2002**, *80* (1), 112.
- (26) Pradhan, B.; Batabyal, S. K.; Pal, A. J. Functionalized Carbon Nanotubes in Donor/acceptor-Type Photovoltaic Devices. *Appl. Phys. Lett.* **2006**, *88* (9), 093106.
- (27) Li, C.; Chen, Y.; Wang, Y.; Iqbal, Z.; Chhowalla, M.; Mitra, S. A Fullerene–single Wall Carbon Nanotube Complex for Polymer Bulk Heterojunction Photovoltaic Cells. *J. Mater. Chem.* **2007**, *17* (23), 2406–2411.
- (28) Chirvase, D.; Parisi, J.; Hummelen, J. C.; Dyakonov, V. Influence of Nanomorphology on the Photovoltaic Action of Polymer–fullerene Composites. *Nanotechnology* **2004**, *15* (9), 1317–1323.
- (29) Ren, S.; Bernardi, M.; Lunt, R. R.; Bulovic, V.; Grossman, J. C.; Gradečak, S. Toward Efficient Carbon nanotube/P3HT Solar Cells: Active Layer Morphology, Electrical, and Optical Properties. *Nano Lett.* **2011**, *11* (12), 5316–5321.
- (30) Bindl, D. J.; Safron, N. S.; Arnold, M. S. Dissociating Excitons Photogenerated in Semiconducting Carbon Nanotubes at Polymeric Photovoltaic Heterojunction Interfaces. *ACS Nano* **2010**, *4* (10), 5657–5664.
- (31) Arnold, M. S.; Zimmerman, J. D.; Renshaw, C. K.; Xu, X.; Lunt, R. R.; Austin, C. M.; Forrest, S. R. Broad Spectral Response Using Carbon Nanotube/Organic

Semiconductor/C 60 Photodetectors. *Nano Lett.* **2009**, *9* (9), 3354–3358.

- (32) Bindl, D. J.; Wu, M. Y.; Prehn, F. C.; Arnold, M. S. Efficiently Harvesting Excitons from Electronic Type-Controlled Semiconducting Carbon Nanotube Films. *Nano Lett.* **2011**, *11* (2), 455–460.
- (33) Bindl, D. J.; Brewer, A. S.; Arnold, M. S. Semiconducting Carbon Nanotube/fullerene Blended Heterojunctions for Photovoltaic near-Infrared Photon Harvesting. *Nano Res.* **2011**, *4* (11), 1174–1179.
- (34) Jain, R. M.; Howden, R.; Tvrdy, K.; Shimizu, S.; Hilmer, A. J.; McNicholas, T. P.; Gleason, K. K.; Strano, M. S. Polymer-Free near-Infrared Photovoltaics with Single Chirality (6,5) Semiconducting Carbon Nanotube Active Layers. *Adv. Mater.* **2012**, *24* (32), 4436–4439.
- (35) Raj, R.; Maroo, S. C.; Wang, E. N. Wettability of Graphene. *Nano Lett.* **2013**, *13* (4), 1509–1515.
- (36) Rafiee, J.; Mi, X.; Gullapalli, H.; Thomas, A. V.; Yavari, F.; Shi, Y.; Ajayan, P. M.; Koratkar, N. a. Wetting Transparency of Graphene. *Nat. Mater.* **2012**, *11* (3), 217–222.
- (37) Wang, S. R.; Zhang, Y.; Abidi, N.; Cabrales, L. Wettability and Surface Free Energy of Graphene Films. *Langmuir* **2009**, *25* (18), 11078–11081.
- (38) Kim, B. H.; Kim, J. Y.; Jeong, S. J.; Hwang, J. O.; Lee, D. H.; Shin, D. O.; Choi, S. Y.; Kim, S. O. Surface Energy Modification by Spin-Cast, Large-Area Graphene Film for Block Copolymer Lithography. *ACS Nano* **2010**, *4* (9), 5464–5470.
- (39) Shin, Y. J.; Wang, Y.; Huang, H.; Kalon, G.; Wee, A. T. S.; Shen, Z.; Bhatia, C. S.; Yang, H. Surface-Energy Engineering of Graphene. *Langmuir* **2010**, *26* (6), 3798–3802.
- (40) Tung, V. C.; Huang, J.-H. J.; Kim, J.; Smith, A. J.; Chu, C.-W.; Huang, J.-H. J. Towards Solution Processed All-Carbon Solar Cells: A Perspective. *Energy Environ. Sci.* **2012**, *5* (7), 7810.
- (41) Tung, V. C.; Huang, J. H.; Tevis, I.; Kim, F.; Kim, J.; Chu, C. W.; Stupp, S. I.; Huang, J. Surfactant-Free Water-Processable Photoconductive All-Carbon Composite. *J. Am. Chem. Soc.* **2011**, *133* (13), 4940–4947.
- (42) Bernardi, M.; Lohrman, J.; Kumar, P. V.; Kirkeminde, A.; Ferralis, N.; Grossman, J. C.; Ren, S. Nanocarbon-Based Photovoltaics. *ACS Nano* **2012**, *6* (10), 8896–8903.
- (43) Ramuz, M. P.; Vosgueritchian, M.; Wei, P.; Wang, C.; Gao, Y.; Wu, Y.; Chen, Y.;

- Bao, Z. Evaluation of Solution-Processable Carbon-Based Electrodes for All-Carbon Solar Cells. *ACS Nano* **2012**, *6* (11), 10384–10395.
- (44) Wang, H.; Koleilat, G. I.; Liu, P.; Jiménez-Osés, G.; Lai, Y.-C.; Vosgueritchian, M.; Fang, Y.; Park, S.; Houk, K. N.; Bao, Z. High-Yield Sorting of Small-Diameter Carbon Nanotubes for Solar Cells and Transistors. *ACS Nano* **2014**, *8* (3), 2609–2617.
- (45) Gong, M.; Shastry, T. A.; Xie, Y.; Bernardi, M.; Jasion, D.; Luck, K. A.; Marks, T. J.; Grossman, J. C.; Ren, S.; Hersam, M. C. Polychiral Semiconducting Carbon Nanotube–Fullerene Solar Cells. *Nano Lett.* **2014**, *14* (9), 5308–5314.
- (46) Lee, J. M.; Park, J. S.; Lee, S. H.; Kim, H.; Yoo, S.; Kim, S. O. Selective Electron- or Hole-Transport Enhancement in Bulk-Heterojunction Organic Solar Cells with N- or B-Doped Carbon Nanotubes. *Adv. Mater.* **2011**, *23* (5), 629–633.
- (47) Robel, I.; Bunker, B. A.; Kamat, P. V. Single-Walled Carbon Nanotube-CdS Nanocomposites as Light-Harvesting Assemblies: Photoinduced Charge-Transfer Interactions. *Adv. Mater.* **2005**, *17* (20), 2458–2463.
- (48) Barazzouk, S.; Hotchandani, S.; Vinodgopal, K.; Kamat, P. V. Single-Wall Carbon Nanotube Films for Photocurrent Generation. A Prompt Response to Visible-Light Irradiation. *J. Phys. Chem. B* **2004**, *108* (44), 17015–17018.
- (49) Landi, B. J.; Castro, S. L.; Ruf, H. J.; Evans, C. M.; Bailey, S. G.; Raffaele, R. P. CdSe Quantum Dot-Single Wall Carbon Nanotube Complexes for Polymeric Solar Cells. *Sol. Energy Mater. Sol. Cells* **2005**, *87* (1-4), 733–746.
- (50) Lee, J. M.; Kwon, B.-H. H.; Park, H. Il; Kim, H.; Kim, M. G.; Park, J. S.; Kim, E. S.; Yoo, S.; Jeon, D. Y.; Kim, S. O. Exciton Dissociation and Charge-Transport Enhancement in Organic Solar Cells with Quantum-dot/N-Doped CNT Hybrid Nanomaterials. *Adv. Mater.* **2013**, *25* (14), 2011–2017.
- (51) Lu, L.; Xu, T.; Chen, W.; Lee, J. M.; Luo, Z.; Jung, I. H.; Park, H. Il; Kim, S. O.; Yu, L. The Role of N-Doped Multiwall Carbon Nanotubes in Achieving Highly Efficient Polymer Bulk Heterojunction Solar Cells. *Nano Lett.* **2013**, *13* (6), 2365–2369.
- (52) Jeon, I.; Kutsuzawa, D.; Hashimoto, Y.; Yanase, T.; Nagahama, T.; Shimada, T.; Matsuo, Y. Multilayered MoS₂ Nanoflakes Bound to Carbon Nanotubes as Electron Acceptors in Bulk Heterojunction Inverted Organic Solar Cells. *Org. Electron.* **2015**, *17*, 275–280.
- (53) Thompson, B. C.; Fréchet, J. M. J. Polymer–Fullerene Composite Solar Cells. *Angew. Chemie Int. Ed.* **2008**, *47* (1), 58–77.

- (54) Nelson, J. Polymer:fullerene Bulk Heterojunction Solar Cells. *Mater. Today* **2011**, *14* (10), 462–470.
- (55) Dennler, G.; Scharber, M. C.; Brabec, C. J. Polymer-Fullerene Bulk-Heterojunction Solar Cells. *Adv. Mater.* **2009**, *21* (13), 1323–1338.
- (56) Zilberberg, K.; Gasse, F.; Pagui, R.; Polywka, A.; Behrendt, A.; Trost, S.; Heiderhoff, R.; Görrn, P.; Riedl, T. Highly Robust Indium-Free Transparent Conductive Electrodes Based on Composites of Silver Nanowires and Conductive Metal Oxides. *Adv. Funct. Mater.* **2014**, *24* (12), 1671–1678.
- (57) Inganäs, O. Organic Photovoltaics: Avoiding Indium. *Nat. Photonics* **2011**, *5* (4), 201–202.
- (58) Yang, M.; Kim, D.; Jha, H.; Lee, K.; Paul, J.; Schmuki, P. Nb Doping of TiO₂ Nanotubes for an Enhanced Efficiency of Dye-Sensitized Solar Cells. *Chem. Commun.* **2011**, *47* (7), 2032–2034.
- (59) Delacou, C.; Jeon, I.; Seo, S.; Nakagawa, T.; Kauppinen, E. I.; Maruyama, S.; Matsuo, Y. Indium Tin Oxide-free Small Molecule Organic Solar Cells using Single-Walled Carbon Nanotube Electrodes. *ECS J. Solid State Sci. Technol.* **2017**, *6* (6) M3181-M3184.
- (60) Sakaguchi, T.; Jeon, I.; Chiba, T.; Shawky, A.; Xiang, R.; Chiashi, S.; Kauppinen, E. I.; Park, N.-G.; Matsuo, Y.; Maruyama S. Single-walled Carbon Nanotube-based Metal-free Perovskite Solar Cells with improved Stability and Efficiency. *J. Mater. Chem. A* **2017** submitted
- (61) Wu, Z.; Chen, Z.; Du, X.; Logan, J. M.; Sippel, J.; Nikolou, M.; Kamaras, K.; Reynolds, J. R.; Tanner, D. B.; Hebard, A. F.; Rinzler, A. G. Transparent, Conductive Carbon Nanotube Films. *Science* **2004**, *305* (5688), 1273–1276.
- (62) Lee, Y. H.; Kim, S. G.; Tománek, D. Catalytic Growth of Single-Wall Carbon Nanotubes: An Ab Initio Study. *Phys. Rev. Lett.* **1997**, *78* (12), 2393–2396.
- (63) Nasibulin, A. G.; Kaskela, A.; Mustonen, K.; Anisimov, A. S.; Ruiz, V.; Kivistö, S.; Rackauskas, S.; Timmermans, M. Y.; Pudas, M.; Aitchison, B.; Kauppinen, M.; Brown, D. P.; Okhotnikov, O. G.; Kauppinen, E. I. Multifunctional Free-Standing Single-Walled Carbon Nanotube Films. *ACS Nano* **2011**, *5* (4), 3214–3221.
- (64) van de Lagemaat, J.; Barnes, T. M.; Rumbles, G.; Shaheen, S. E.; Coutts, T. J.; Weeks, C.; Levitsky, I.; Peltola, J.; Glatkowski, P. Organic Solar Cells with Carbon Nanotubes Replacing In₂O₃:Sn as the Transparent Electrode. *Appl. Phys. Lett.* **2006**, *88* (23), 233503.

- (65) Ahn, N.; Jeon, I.; Yoon, J.; Kauppinen, E. I.; Yutaka, M.; Maruyama, S.; Choi, M. Carbon-Sandwiched Perovskite Solar Cell. *J. Mater. Chem. A* **2017** under review
- (66) Schneider, J.; Rohner, P.; Thureja, D.; Schmid, M.; Galliker, P.; Poulikakos, D. Electrohydrodynamic NanoDrip Printing of High Aspect Ratio Metal Grid Transparent Electrodes. *Adv. Funct. Mater.* **2016**, *26*, 833–840.
- (67) Langley D, Giusti G, Mayousse C, Celle C, Bellet D, Simonato JP (2013) Flexible transparent conductive materials based on silver nanowire networks: a review. *Nanotechnology* 24(45): 452001
- (68) Cao W, Li J, Chen H, Xue J (2014) Transparent electrodes for organic optoelectronic devices: a review. *J. Photonics Energy* 4: 040990
- (69) Bae S, Kim H, Lee Y, Xu X, Park JS, Zheng Y, Balakrishnan J., Lei T, Kim HR, Song YI, Kim YJ, Kim KS, Ozyilmaz B, Ahn JH, Hong BH, Iijima S (2010) Roll-to-roll production of 30-inch graphene films for transparent electrodes. *Nat. Nanotechnol* 5: 574-578
- (70) Hou PX, Yu B, Su Y, Shi C, Zhang LL, Liu C, Li SS, Du JH, Cheng HM (2014) Double-wall carbon nanotube transparent conductive films with excellent performance. *J. Mater. Chem. A* 2: 1159-1164
- (71) Hecht DS, Heintz AM, Lee R, Hu L, Moore B, Cucksey C, Risser S (2011) High conductivity transparent carbon nanotube films deposited from superacid. *Nanotechnology* 22: 075201
- (72) Tune, D. D.; Flavel, B. S.; Krupke, R.; Shapter, J. G. Carbon Nanotube-Silicon Solar Cells. *Adv. Energy Mater.* **2012**, *2* (9), 1043–1055.
- (73) Jung, Y.; Li, X.; Rajan, N. K.; Taylor, A. D.; Reed, M. A. Record High Efficiency Single-Walled Carbon Nanotube/Silicon P – N Junction Solar Cells. *Nano Lett.* **2013**, *13* (1), 95–99.
- (74) Wei, J.; Jia, Y.; Shu, Q.; Gu, Z.; Wang, K.; Zhuang, D.; Zhang, G.; Wang, Z.; Luo, J.; Cao, A.; Wu, D. Double-Walled Carbon Nanotube Solar Cells. *Nano Lett.* **2007**, *7* (8), 2317-2321.
- (75) Wenham, S. R.; Green, M. A. Silicon Solar Cells. *Prog. Photovoltaics Res. Appl.* **1996**, *4* (1), 3–33.
- (76) Song, Y.; Li, X.; Mackin, C.; Zhang, X.; Fang, W.; Palacios, T.; Zhu, H.; Kong, J. Role of Interfacial Oxide in High-Efficiency Graphene–Silicon Schottky Barrier Solar Cells. *Nano Lett.* **2015**, *15* (3), 2104-2110.
- (77) Shi, E.; Zhang, L.; Li, Z.; Li, P.; Shang, Y.; Jia, Y.; Wei, J.; Wang, K.; Zhu, H.;

- Wu, D.; Zhang, S.; Cao, A. TiO₂-Coated Carbon Nanotube-Silicon Solar Cells with Efficiency of 15%. *Sci. Rep.* **2012**, *2*, 884.
- (78) Anderson, W. A. An 8% Efficient Layered Schottky-Barrier Solar Cell. *J. Appl. Phys.* **1974**, *45* (9), 3913.
- (79) Tung, R. T. Recent Advances in Schottky Barrier Concepts. *Mater. Sci. Eng. R Reports* **2001**, *35* (1-3), 1–138.
- (80) Jia, Y.; Wei, J.; Wang, K.; Cao, A.; Shu, Q.; Gui, X.; Zhu, Y.; Zhuang, D.; Zhang, G.; Ma, B.; Wang, L.; Liu, W.; Wang, Z.; Luo, J.; Wu, D. Nanotube-silicon heterojunction solar cells. *Adv. Mater.* **2008**, *20* (23) 4594.
- (81) Li, Z.; Kunets, V. P.; Saini, V.; Xu, Y.; Dervishi, E.; Salamo, G. J.; Biris, A. R.; Biris, A. S. SOCl₂ Enhanced Photovoltaic Conversion of Single Wall Carbon Nanotube/n-Silicon Heterojunctions. *Appl. Phys. Lett.* **2008**, *93* (24), 243117.
- (82) Li, Z.; Kunets, V. P.; Saini, V.; Xu, Y.; Dervishi, E.; Salamo, G. J.; Biris, A. R.; Biris, A. S. Light-Harvesting Using High Density P -Type Single Wall Carbon Nanotube/ N -Type Silicon Heterojunctions. *ACS Nano* **2009**, *3* (6), 1407–1414.
- (83) Li, Z.; Jia, Y.; Wei, J.; Wang, K.; Shu, Q.; Gui, X.; Zhu, H.; Cao, A.; Wu, D. Large Area, Highly Transparent Carbon Nanotube Spiderwebs for Energy Harvesting. *J. Mater. Chem.* **2010**, *20* (34), 7236.
- (84) Blackburn, J. L.; Barnes, T. M.; Beard, M. C.; Kim, Y.-H.; Tenent, R. C.; McDonald, T. J.; To, B.; Coutts, T. J.; Heben, M. J. Transparent Conductive Single-Walled Carbon Nanotube Networks with Precisely Tunable Ratios of Semiconducting and Metallic Nanotubes. *ACS Nano* **2008**, *2* (6), 1266–1274.
- (85) Ong, P.-L.; Euler, W. B.; Levitsky, I. a. Hybrid Solar Cells Based on Single-Walled Carbon nanotubes/Si Heterojunctions. *Nanotechnology* **2010**, *21* (10), 105203.
- (86) Wadhwa, P.; Liu, B.; McCarthy, M. A.; Wu, Z.; Rinzler, A. G. Electronic Junction Control in a Nanotube-Semiconductor Schottky Junction Solar Cell. *Nano Lett.* **2010**, *10* (12), 5001–5005.
- (87) Jia, Y.; Cao, A.; Bai, X.; Li, Z.; Zhang, L.; Guo, N.; Wei, J.; Wang, K.; Zhu, H.; Wu, D.; Ajayan, P. M. Achieving High Efficiency Silicon-Carbon Nanotube Heterojunction Solar Cells by Acid Doping. *Nano Lett.* **2011**, *11* (5), 1901–1905.
- (88) Jia, Y.; Li, P.; Gui, X.; Wei, J.; Wang, K.; Zhu, H.; Wu, D.; Zhang, L.; Cao, A.; Xu, Y. Encapsulated Carbon Nanotube-Oxide-Silicon Solar Cells with Stable 10% Efficiency. *Appl. Phys. Lett.* **2011**, *98* (13).

- (89) Wadhwa, P.; Seol, G.; Petterson, M. K.; Guo, J.; Rinzler, A. G. Electrolyte-Induced Inversion Layer Schottky Junction Solar Cells. *Nano Lett.* **2011**, *11* (6), 2419–2423.
- (90) Chen, W.; Seol, G.; Rinzler, A. G.; Guo, J. Carrier Dynamics and Design Optimization of Electrolyte-Induced Inversion Layer Carbon Nanotube-Silicon Schottky Junction Solar Cell. *Appl. Phys. Lett.* **2012**, *100* (10), 103503.
- (91) Kozawa, D.; Hiraoka, K.; Miyauchi, Y.; Mouri, S.; Matsuda, K. Analysis of the Photovoltaic Properties of Single-Walled Carbon Nanotube/Silicon Heterojunction Solar Cells. *Appl. Phys. Express* **2012**, *5* (4), 042304.
- (92) Li, X.; Jung, Y.; Sakimoto, K.; Goh, T.-H.; Reed, M. A.; Taylor, A. D. Improved efficiency of smooth and aligned single walled carbon nanotube/silicon hybrid solar cells. *Energ. Environ. Sci.* **2013**, *6* (3), 879–887.
- (93) Cui, K.; Chiba, T.; Omiya, S.; Thurakitseree, T.; Zhao, P.; Fujii, S.; Kataura, H.; Einarsson, E.; Chiashi, S.; Maruyama, S. Self-Assembled Microhoneycomb Network of Single-Walled Carbon Nanotubes for Solar Cells. *J. Phys. Chem. Lett.* **2013**, *4* (15), 2571–2576.
- (94) Xu, W.; Deng, B.; Shi, E.; Wu, S.; Zou, M.; Yang, L.; Wei, J.; Peng, H.; Cao, A. Comparison of Nanocarbon–Silicon Solar Cells with Nanotube–Si or Graphene–Si Contact. *ACS Appl. Mater. Interfaces* **2015**, *7* (31), 17088–17094.
- (95) Cui, K.; Anisimov, A. S.; Chiba, T.; Fujii, S.; Kataura, H.; Nasibulin, A. G.; Chiashi, S.; Kauppinen, E. I.; Maruyama, S. Air-Stable High-Efficiency Solar Cells with Dry-Transferred Single-Walled Carbon Nanotube Films. *J. Mater. Chem. A* **2014**, *2* (29), 11311–11318.
- (96) Li, Z.; Saini, V.; Dervishi, E.; Kunets, V. P.; Zhang, J.; Xu, Y.; Biris, A. R.; Salamo, G. J.; Biris, A. S. Polymer Functionalized N-Type Single Wall Carbon Nanotube Photovoltaic Devices. *Appl. Phys. Lett.* **2010**, *96* (3).
- (97) Wang, F.; Kozawa, D.; Miyauchi, Y.; Hiraoka, K.; Mouri, S.; Ohno, Y.; Matsuda, K. Considerably Improved Photovoltaic Performance of Carbon Nanotube-Based Solar Cells Using Metal Oxide Layers. *Nat. Commun.* **2015**, *6*, 6305.
- (98) Dou, L.; You, J.; Yang, J.; Chen, C.; He, Y.; Murase, S.; Moriarty, T.; Emery, K.; Li, G.; Yang, Y. Tandem Polymer Solar Cells Featuring a Spectrally Matched Low-Bandgap Polymer. *Nat. Photonics* **2012**, *6* (3), 180–185.
- (99) Angmo, D.; Krebs, F. C. Flexible ITO-Free Polymer Solar Cells. *J. Appl. Polym. Sci.* **2013**, *129* (1), 1–14.

- (100) Jariwala, D.; Sangwan, V. K.; Lauhon, L. J.; Marks, T. J.; Hersam, M. C. Carbon Nanomaterials for Electronics, Optoelectronics, Photovoltaics, and Sensing. *Chem. Soc. Rev.* **2013**, *42* (7), 2824–2860.
- (101) Liu, Y.; Wan, X.; Wang, F.; Zhou, J.; Long, G.; Tian, J.; You, J.; Yang, Y.; Chen, Y. Spin-Coated Small Molecules for High Performance Solar Cells. *Adv. Energy Mater.* **2011**, *1* (5), 771–775.
- (102) Li, S.-S.; Chen, C.-W. Polymer–metal-Oxide Hybrid Solar Cells. *J. Mater. Chem. A* **2013**, *1* (36), 10574.
- (103) Rowell, M. W.; Topinka, M. A.; McGehee, M. D.; Prall, H.-J.; Dennler, G.; Sariciftci, N. S.; Hu, L.; Gruner, G. Organic Solar Cells with Carbon Nanotube Network Electrodes. *Appl. Phys. Lett.* **2006**, *88* (23), 233506.
- (104) Gomez De Arco, L.; Zhang, Y.; Schlenker, C. W.; Ryu, K.; Thompson, M. E.; Zhou, C. Continuous, Highly Flexible, and Transparent Graphene Films by Chemical Vapor Deposition for Organic Photovoltaics. *ACS Nano* **2010**, *4* (5), 2865–2873.
- (105) Unalan, H. E.; Hiralal, P.; Kuo, D.; Parekh, B.; Amaratunga, G.; Chhowalla, M. Flexible Organic Photovoltaics from Zinc Oxide Nanowires Grown on Transparent and Conducting Single Walled Carbon Nanotube Thin Films. *J. Mater. Chem.* **2008**, *18* (48), 5909.
- (106) Kymakis, E.; Klapsis, G.; Koudoumas, E.; Stratakis, E.; Kornilios, N.; Vidakis, N.; Franghiadakis, Y. Carbon nanotube/PEDOT:PSS Electrodes for Organic Photovoltaics. *Eur. Phys. J. Appl. Phys.* **2006**, *36* (3), 257–259.
- (107) Kim, S.; Yim, J.; Wang, X.; Bradley, D. D. C.; Lee, S.; DeMello, J. C. Spin- and Spray-Deposited Single-Walled Carbon-Nanotube Electrodes for Organic Solar Cells. *Adv. Funct. Mater.* **2010**, *20* (14), 2310–2316.
- (108) Tyler, T. P.; Brock, R. E.; Karmel, H. J.; Marks, T. J.; Hersam, M. C. Electronically Monodisperse Single-Walled Carbon Nanotube Thin Films as Transparent Conducting Anodes in Organic Photovoltaic Devices. *Adv. Energy Mater.* **2011**, *1* (5), 785–791.
- (109) Salvatierra, R. V.; Cava, C. E.; Roman, L. S.; Zarbin, A. J. G. ITO-Free and Flexible Organic Photovoltaic Device Based on High Transparent and Conductive Polyaniline/Carbon Nanotube Thin Films. *Adv. Funct. Mater.* **2013**, *23* (12), 1490–1499.
- (110) Jeon, I.; Cui, K.; Chiba, T.; Anisimov, A.; Nasibulin, A. G.; Kauppinen, E. I.; Maruyama, S.; Matsuo, Y. Direct and Dry Deposited Single-Walled Carbon

- Nanotube Films Doped with MoO₃ as Electron-Blocking Transparent Electrodes for Flexible Organic Solar Cells. *J. Am. Chem. Soc.* **2015**, *137* (25), 7982–7985.
- (111) Hellstrom, S. L.; Vosgueritchian, M.; Stoltenberg, R. M.; Irfan, I.; Hammock, M.; Wang, Y. B.; Jia, C.; Guo, X.; Gao, Y.; Bao, Z. Strong and Stable Doping of Carbon Nanotubes and Graphene by MoO₃ for Transparent Electrodes. *Nano Lett.* **2012**, *12* (7), 3574–3580.
- (112) Shin, D.-W.; Lee, J. H.; Kim, Y.-H.; Yu, S. M.; Park, S.-Y.; Yoo, J.-B. A Role of HNO₃ on Transparent Conducting Film with Single-Walled Carbon Nanotubes. *Nanotechnology* **2009**, *20* (47), 475703.
- (113) Deb, S. K. Optical Properties and Color-Center Formation in Thin Films of Molybdenum Trioxide. *J. Appl. Phys.* **1966**, *37* (13), 4818.
- (114) Jeon, I.; Delacou, C.; Kaskela, A.; Kauppinen, I. E.; Maruyama, S.; Matsuo, Y. Metal-electrode-free Window-like Organic Solar Cells with p-Doped Carbon Nanotube Thin-film Electrodes. *Sci. Rep.* **2016**, *6*, 31348.
- (115) Chappel, S.; Chen, S.-G.; Zaban, A. TiO₂-Coated Nanoporous SnO₂ Electrodes for Dye-Sensitized Solar Cells. *Langmuir* **2002**, *18* (8), 3336–3342.
- (116) Suzuki, K.; Yamaguchi, M.; Kumagai, M.; Yanagida, S. Application of Carbon Nanotubes to Counter Electrodes of Dye-Sensitized Solar Cells. *Chem. Lett.* **2003**, *32* (1), 28–29.
- (117) Kay, A.; Grätzel, M. Low Cost Photovoltaic Modules Based on Dye Sensitized Nanocrystalline Titanium Dioxide and Carbon Powder. *Sol. Energy Mater. Sol. Cells* **1996**, *44* (1), 99–117.
- (118) Jang, S.-R.; Vittal, R.; Kim, K.-J. Incorporation of Functionalized Single-Wall Carbon Nanotubes in Dye-Sensitized TiO₂ Solar Cells. *Langmuir* **2004**, *20* (22), 9807–9810.
- (119) Kongkanand, A.; Martínez Domínguez, R.; Kamat, P. V. Single Wall Carbon Nanotube Scaffolds for Photoelectrochemical Solar Cells. Capture and Transport of Photogenerated Electrons. *Nano Lett.* **2007**, *7* (3), 676–680.
- (120) Lee, T. Y.; Alegaonkar, P. S.; Yoo, J.-B. Fabrication of Dye Sensitized Solar Cell Using TiO₂ Coated Carbon Nanotubes. *Thin Solid Films* **2007**, *515* (12), 5131–5135.
- (121) Snaith, H. J. Perovskites: The Emergence of a New Era for Low-Cost, High-Efficiency Solar Cells. *J. Phys. Chem. Lett.* **2013**, *4* (21), 3623–3630.
- (122) Green, M. A.; Ho-Baillie, A.; Snaith, H. J. The Emergence of Perovskite Solar

Cells. *Nat. Photonics* **2014**, *8* (7), 506–514.

- (123) McGehee, M. D. Perovskite Solar Cells: Continuing to Soar. *Nat. Mater.* **2014**, *13* (9), 845–846.
- (124) Jeon, I.; Chiba, T.; Delacou, C.; Guo, Y.; Kaskela, A.; Reynaud, O.; Kauppinen, E. I.; Maruyama, S.; Matsuo, Y. Single-Walled Carbon Nanotube Film as Electrode in Indium-Free Planar Heterojunction Perovskite Solar Cells: Investigation of Electron-Blocking Layers and Dopants. *Nano Lett.* **2015**, *15* (10), 6665–6671.
- (125) Li, Z.; Kulkarni, S. A.; Boix, P. P.; Shi, E.; Cao, A.; Fu, K.; Batabyal, S. K.; Zhang, J.; Xiong, Q.; Wong, L. H.; Mathews, N.; Mhaisalkar, S. G. Laminated Carbon Nanotube Networks for Metal Electrode-Free Efficient Perovskite Solar Cells. *ACS Nano* **2014**, *8* (7), 6797–6804.
- (126) Wang, X.; Li, Z.; Xu, W.; Kulkarni, S. A.; Batabyal, S. K.; Zhang, S.; Cao, A.; Wong, L. H. TiO₂ Nanotube Arrays Based Flexible Perovskite Solar Cells with Transparent Carbon Nanotube Electrode. *Nano Energy* **2015**, *11*, 728–735.
- (127) Aitola, K.; Sveinbjörnsson, K.; Correa-Baena, J.-P.; Kaskela, A.; Abate, A.; Tian, Y.; Johansson, E. M. J.; Grätzel, M.; Kauppinen, E. I.; Hagfeldt, A.; Boschloo, G. Carbon Nanotube-Based Hybrid Hole-Transporting Material and Selective Contact for High Efficiency Perovskite Solar Cells. *Energy Environ. Sci.* **2016**, *9* (2), 461–466.
- (128) Habisreutinger, S. N.; Leijtens, T.; Eperon, G. E.; Stranks, S. D.; Nicholas, R. J.; Snaith, H. J. Carbon Nanotube/Polymer Composites as a Highly Stable Hole Collection Layer in Perovskite Solar Cells. *Nano Lett.* **2014**, *14* (10), 5561–5568.
- (129) Jeon, I.; Yoon, J.; Ahn, N.; Atwa, M.; Delacou, C.; Sota, M.; Kauppinen, E. I.; Choi, M.; Maruyama, S.; Matsuo, Y. Carbon Nanotubes versus Graphene as Flexible Transparent Electrodes in Perovskite Solar Cells. *J. Phys. Chem. Lett.* **2017**, *8*, 5395–5401.
- (130) Jeon, I.; Seo, S.; Sato, Y.; Delacou, C.; Suenaga, K.; Kauppinen, E. I.; Maruyama, S.; Matsuo, Y. Perovskite Solar Cells using Carbon Nanotubes as both Cathode and Anode Electrodes' *J. Phys. Chem. C* **2017**, *21* (46) 25743–25749.
- (131) Choe, M.; Lee, B. H.; Jo, G.; Park, J.; Park, W.; Lee, S.; Hong, W. K.; Seong, M. J.; Kahng, Y. H.; Lee, K.; Lee, T. Efficient Bulk-Heterojunction Photovoltaic Cells with Transparent Multi-Layer Graphene Electrodes. *Org. Electron. physics, Mater. Appl.* **2010**, *11* (11), 1864–1869.
- (132) Du, J.; Pei, S.; Ma, L.; Cheng, H.-M. 25th Anniversary Article: Carbon Nanotube-

and Graphene-Based Transparent Conductive Films for Optoelectronic Devices. *Adv. Mater.* **2014**, *26* (13), 1958–1991.

- (133) Jo, G.; Choe, M.; Lee, S.; Park, W.; Kahng, Y. H.; Lee, T. The Application of Graphene as Electrodes in Electrical and Optical Devices. *Nanotechnology* **2012**, *23* (11), 112001.